to comprise an additional related pair (1253 and 1001) of around 40 kDa and a single spot (1119) of around 28 kDa. Because these two presumed proteins are present at substantially lower abundances than 413, and because the cytosolic HMG-CoA synthase is reported to consist of only one type of polypeptide, they are likely to represent other, very tightly coregulated enzymes. A second group of six spots was selected based on a regulatory pattern close to the inverse of that for spot 413 (MSN's 34, 79, 178, 182, 204, 347; data not shown). For these proteins, the lowest level of expression occurs with exposure to lovastatin plus cholestyramine and the highest level upon exposure to the high-cholesterol diet. Spots 182 and 79 are highly correlated and lie about one charge apart at the same molecular weight; they may thus be isoforms of a single protein. The other four spots probably represent additional enzymes or subunits.

3.3.2 MSN 235 and coregulated spots

A third group of five spots, mainly comprised of mitochondrial proteins including putative mitochondrial HMG-CoA synthase spots, showed a modest induction by lovastatin alone, but little or no effect with any of the other treatments (including the combination of lovastatin and cholestyramine; Fig. 12). This result is intriguing because lovastatin was expected to affect only the regulation of enzymes of cholesterol synthesis, which is entirely extra-mitochondrial. Three of the spots (235, 134, 144) form a closely-packed triad at approximately 30 kDa and are likely to represent isoforms of one protein. All three spots are stained by an antibody to the mitochondrial form of HMG-CoA synthase obtained from Dr. Greenspan. Subcellular fractionation indicates a mitochondrial location. The other two spots (633 at about 38 kDa and 724 at about 69 kDa) are each present at lower abundance than the members of the triad.

3.3.3 An example of an anti-synergistic effect

A sixth spot (367) shows strong induction by lovastatin (two- to threefold), and about half as much induction with lovastatin plus cholestyramine, but without sharing the animal-animal heterogeneity pattern of the 235-set (Fig. 13). This protein is also mitochondrial, and represents the clearest example of an anti-synergistic effect of lovastatin and cholestyramine. The existence of such an effect demonstrates that lovastatin and cholestyramine do not act exclusively through the same regulatory pathway.

3.3.4 Complexity of the cholesterol synthesis pathway

Taken together, these results suggest that treatment with lovastatin alone can affect both cytosolic and mitochondrial pathways using HMG-CoA, while cholestyramine, on the other hand, either alone or in combination with lovastatin, produces a strong effect on the putative cytosolic pathway, but little or no effect on the putative mitochondrial pathway. An explanation for this difference may lie in lovastatin's effect on levels of HMG-CoA and related precursor compounds that are exchanged between the cytosol and the mitochondrion, whereas cholestyramine should affect only the cytosolic pathways directly controlled by cholesterol and bile acid levels. It remains to be explained why some proteins of the putative mitochondrial pathway are so much more variable in their expression in all groups. An examination of all the coregulated groups suggests that quantitative statistical techniques can extract a wealth of interesting information from large sets of reproducible gels. The abundance of spots in the 413 coregulation group, for example, shows an amazing level of concordance in their relative expression among the five individuals of the lovastatin and cholestyramine treatment group. This effect is not due to differences in total protein loading, since they have already been removed by scaling, and since proteins with quite different regulation patterns can be demonstrated (e.g., Fig. 13). Such effects raise the possibility that many gene coregulation sets may be revealed through the study of a sufficiently large population of control animals (*i.e.*, without any experimental manipulation). This approach, exploiting natural biological variation in protein expression instead of drug effects, offers an important incentive for the construction of a large library of control animal patterns.

4 Conclusions

Because of the widespread use of rat liver in both basic biochemistry and in toxicology, there is a long-term need for a comprehensive database of liver proteins. The rat liver master pattern presented here has proven to be an accurate representation of this system, having been matched to more than 700 gels to date. As the number of proteins identified and the number of compounds tested for gene expression effects grows, we expect this database to contribute valuable insights into gene regulation. Its practical utility in several areas of mechanistic toxicology is already being demonstrated.

Received September 11, 1991

5 References

[1] O'Farrell, P., *J. Biol. Chem.* 1975, *250*, 4007–4021.
[2] Klose, J., *Humangenetik* 1975, *26*, 231–243.
[3] Scheele, G. A., *J. Biol. Chem.* 1975, *250*, 5375–5385.
[4] Iborra, G. and Buhler, J. M., *Anal. Biochem.* 1976, *74*, 503–511.
[5] Anderson, N. G. and Anderson, N. L., *Behring. Inst. Mitt.* 1979, *63*, 169–210.
[6] Anderson, N. G. and Anderson, N. L., *Clin. Chem.* 1982, *28*, 739–748.
[7] Heydorn, W. E., Creed, G. J. and Jacobowitz, D. M., *J. Pharmacol. Exp. Therap.* 1984, *229*, 622–628.
[8] Anderson, N. L., Nance, S. L., Tollaksen, S. L., Giere, F. A. and Anderson, N. G., *Electrophoresis* 1985, *6*, 592–599.
[9] Racine, R. R. and Langley, C. H., *Biochem. Genet.* 1980, *18*, 185–197.
[10] Klose, J., *Mol. Evol.* 1982, *18*, 315–328.
[11] Neel, J. V., Baier, L., Hanash, S. and Erickson, R. P., *J. Hered.* 1985, *76*, 314–320.
[12] Marshall, R. R., Raj, A. S., Grant, F. J. and Heddle, J. A., *Can. J. Genet. Cytol.* 1983, *25*, 457–446.
[13] Taylor, J., Anderson, N. L., Anderson, N. G., Gemmell, A., Giometti, C. S., Nance, S. L. and Tollaksen, S. L., in: Dunn, M. J. (Ed.), *Electrophoresis '86*, Verlag Chemie, Weinheim 1986, pp. 583–587.
[14] Giometti, C. S., Gemmell, M. A., Nance, S. L., Tollaksen, S. L. and Taylor, J., *J. Biol. Chem.* 1987, *262*, 12764–12767.
[15] Anderson, N. L., Giere, F. A., Nance, S. L., Gemmell, M. A., Tollaksen, S. L. and Anderson, N. G., in: Galteau, M.-M. and Siest, G. (Eds.), *Progrès Récents en Electrophorèse Bidimensionelle*, Presses Universitaires de Nancy, Nancy 1986, pp. 253–260.
[16] Anderson, N. L., Swanson, M., Giere, F. A., Tollaksen, S., Gemmell, A., Nance, S. L. and Anderson, N. G., *Electrophoresis* 1986, *7*, 44–48.

Anderson, N. L., Giere, F. A., Nance, S. L., Gemmell, M. A., Tollaksen, S. L. and Anderson, N. G., *Fundam. Appl. Toxicol.* 1987, *8*, 39–50.
Anderson, N. L., in: *New Horizons in Toxicology*, Eli Lilly Symposium, 1991, in press.
Antoine, B., Rahimi-Pour, A., Siest, G., Magdalou, J. and Galteau, M. M., *Cell. Biochem. Funct.* 1987, *5*, 217–231.
Elliott, B. M., Ramasamy, R., Stonard, M. D. and Spragg, S. P. *Biochim. Biophys. Acta* 1986, *876*, 135–140.
Huber, B. E., Heilman, C. A., Wirth, P. J., Miller, M. J. and Thorgeirsson, S. S., *Hepatology* 1986, *6*, 206–219.
Wirth, P. J. and Vesterberg, O., *Electrophoresis* 1988, *9*, 47–53.
Witzmann, F. A. and Parker, D. N., *Toxicol. Lett.* 1991, *57*, 29–36.
Rampersaud, A., Waxman, D. J., Ryan, D. E., Levin, W. and Walz, F. G., Jr., *Arch. Biochem. Biophys.* 1985, *243*, 174–183.
Vlasuk, G. P. and Walz, F. G., Jr., *Anal. Biochem.* 1980, *105*, 112–120.
Anderson, N. G. and Anderson, N. L., *Anal. Biochem.* 1978, *85*, 331–340.
Anderson, N. L. and Anderson, N. G., *Anal. Biochem.* 1978, *85*, 341–354.
Anderson, L., Hofmann, J.-P., Anderson, E., Walker, B. and Anderson, N. G., in: Endler, A. T. and Hanash, S. (Eds.), *Two-Dimensional Electrophoresis*, VCH Verlagsgesellschaft, Weinheim 1989, pp. 288–297.
Anderson, L., *Two-Dimensional Electrophoresis: Operation of the ISO-DALT® System*. Large Scale Biology Press, Washington, DC 1988, ISBN 0-945532-00-8, 170pp.
Neuhoff, V., Stamm, R. and Eibl, H., *Electrophoresis* 1985, *6*, 427–448.
[31] Neuhoff, V., Arold, N., Taube, D. and Ehrhardt, W., *Electrophoresis* 1988, *9*, 255–262.
[32] Anderson, N. L. and Hickman, B. J., *Anal. Biochem.* 1979, *93*, 312–320.
[33] Sidman, K. E., George, D. E., Barker, W. C. and Hunt, L. T., *Nucl. Acids Res.* 1988, *16*, 1869–1871.
[34] Taylor, J., Anderson, N. L., Coulter, B. P., Scandora, A. E. and Anderson, N. G., in: Radola, B. J. (Ed.), *Electrophoresis '79*, de Gruyter, Berlin 1980, pp. 329–339.
[35] Taylor, J., Anderson, N. L. and Anderson, N. G., in: Allen, R. C. and Arnaud, P. (Eds.), *Electrophoresis '81*, de Gruyter, Berlin 1981, pp. 383–400.
[36] Anderson, N. L., Taylor, J., Scancora, A. E., Coulter, B. P. and Anderson, N. G., *Clin. Chem.* 1981, *27*, 1807–1820.
[37] Taylor, J., Anderson, N. L., Scandora, A. E., Jr., Willard, K. E. and Anderson, N. G., *Clin. Chem.* 1982, *28*, 861–866.
[38] Taylor, J., Anderson, N. L. and Anderson, N. G., *Electrophoresis* 1983, *4*, 338–345.
[39] Anderson, N. L. and Taylor, J., in: *Proceedings of the Fourth Annual Conference and Exposition of the National Computer Graphics Association*, Chicago, June 26–30, 1983, pp. 69–76.
[40] Anderson, N. L., Hofmann, J.-P., Gemmell, A. and Taylor, J., *Clin. Chem.* 1984, *30*, 2031–2036.
[41] Anderson, L., in: Schafer-Nielsen, C. (Ed.), *Electrophoresis '88*, VCH Verlagsgesellschaft, Weinheim 1988, pp. 313–321.
[42] Neidhardt, F. C., Appleby, D. A., Sankar, P., Hutton, M. E. and Phillips, T. A., *Electrophoresis* 1989, *10*, 116–121.
[43] Gil, G., Goldstein, J. L., Slaughter, C. A. and Brown, M. S., *J. Biol. Chem.* 1986, *261*, 3710–3716.

6 Addendum 1: Figures 1–13

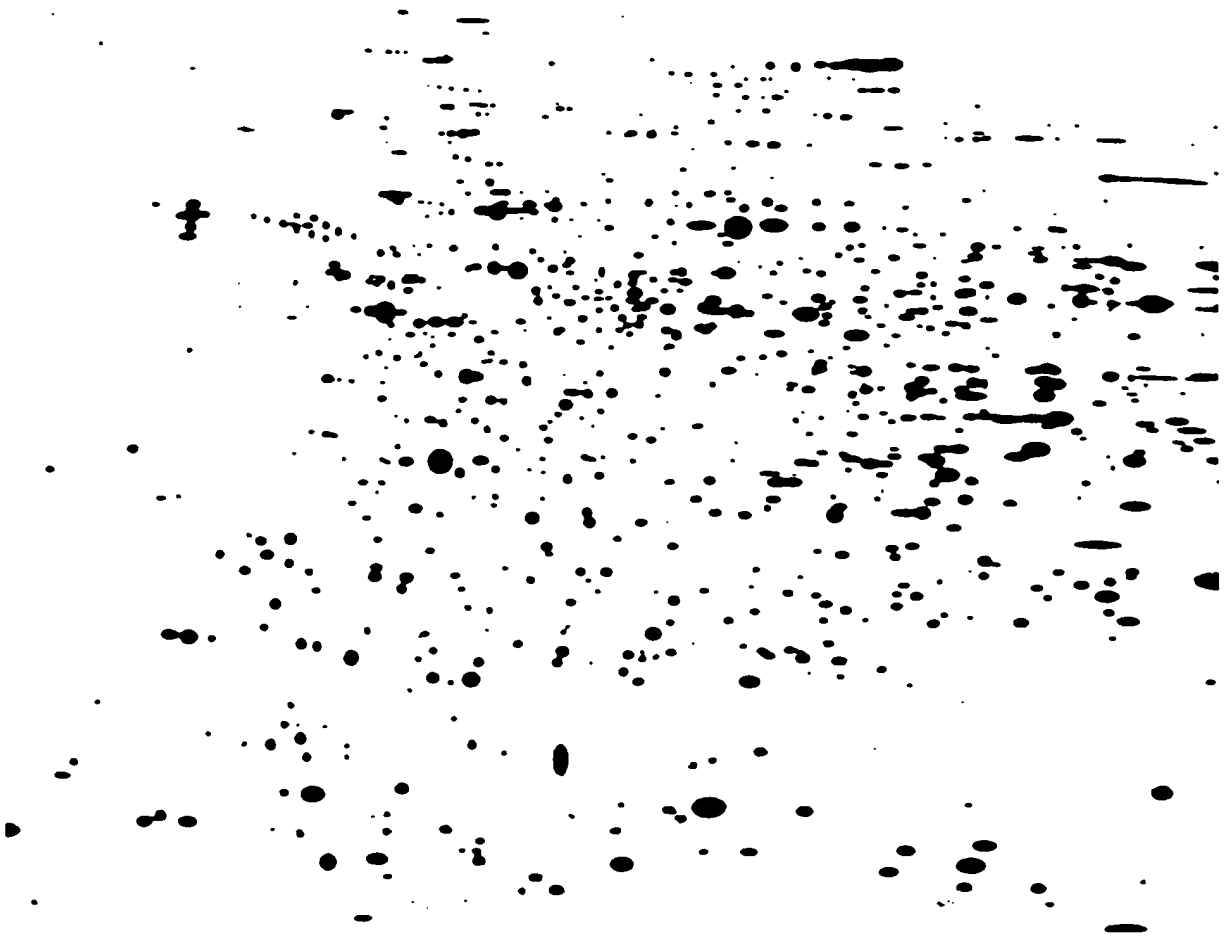

Figure 1. Synthetic representation of the standard rat liver 2-D master pattern, rendered as a greyscale image using a videoprinter.

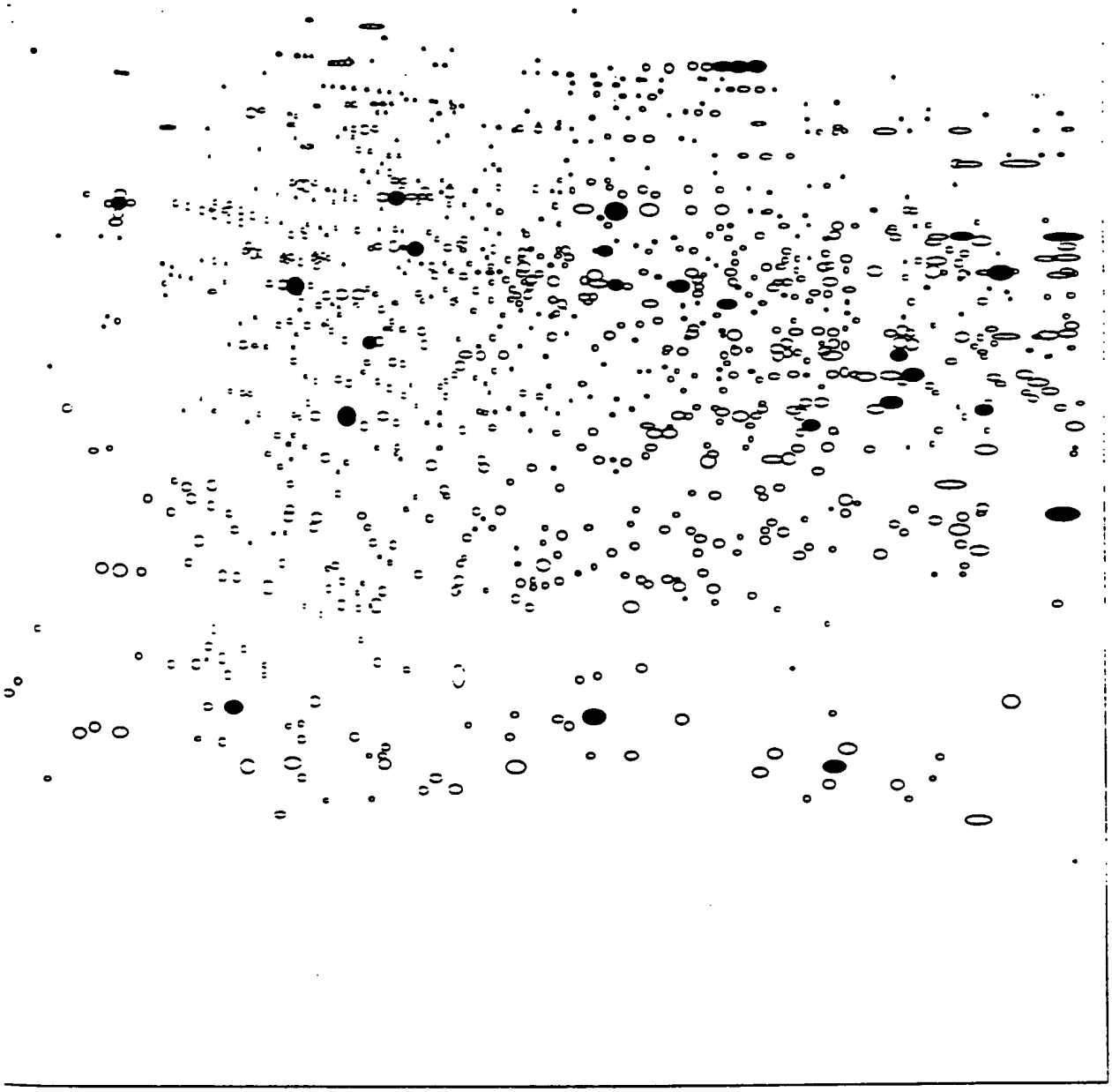

re 2. Schematic representation of the master pattern (the same as Fig. 1), useful as an aid in relating specific areas of Fig. 1 and the following detailed lrants.

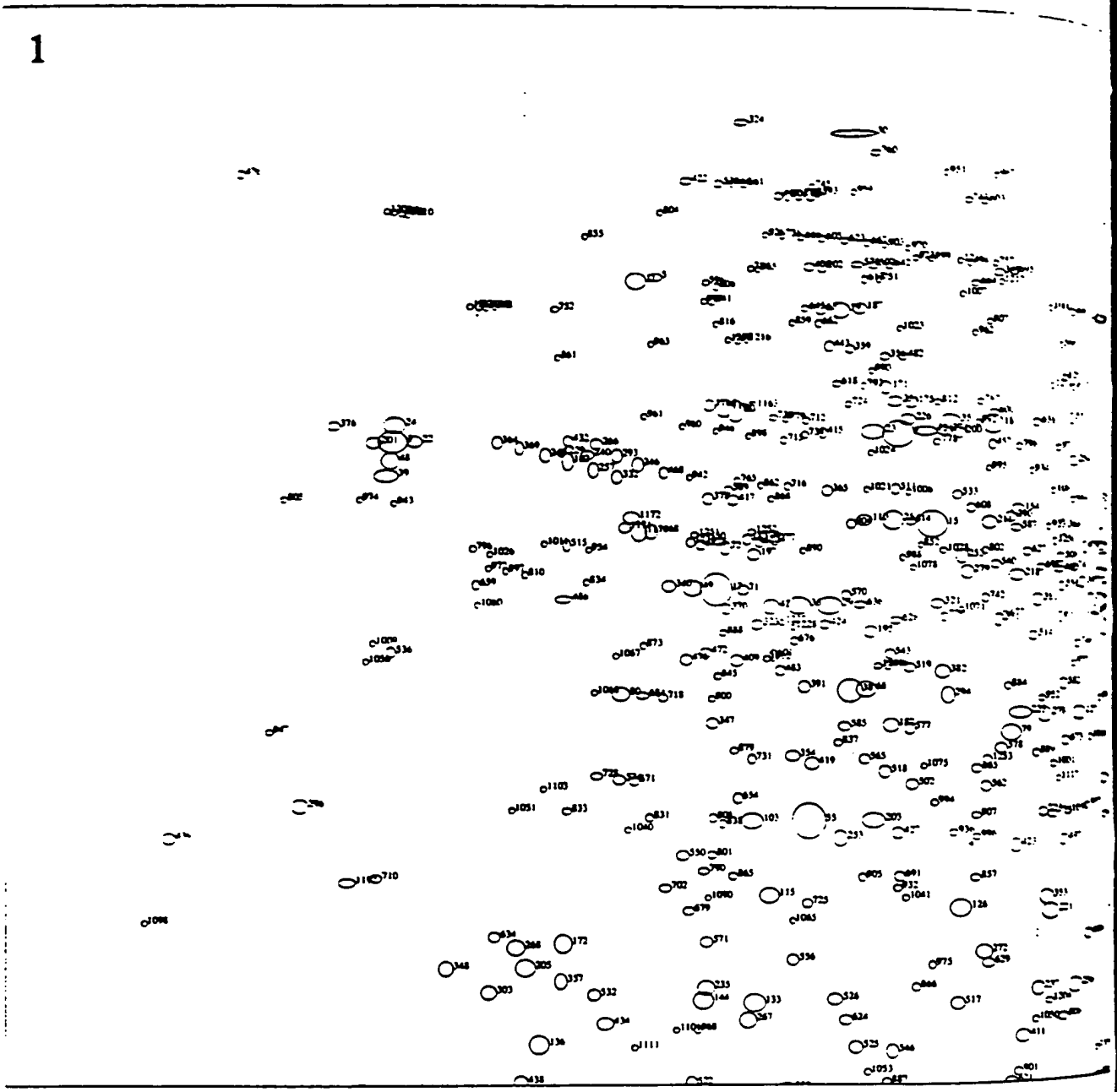

Figure 3. Upper left (high molecular weight, acidic) quadrant (#1) of the rat liver map, showing spot numbers.

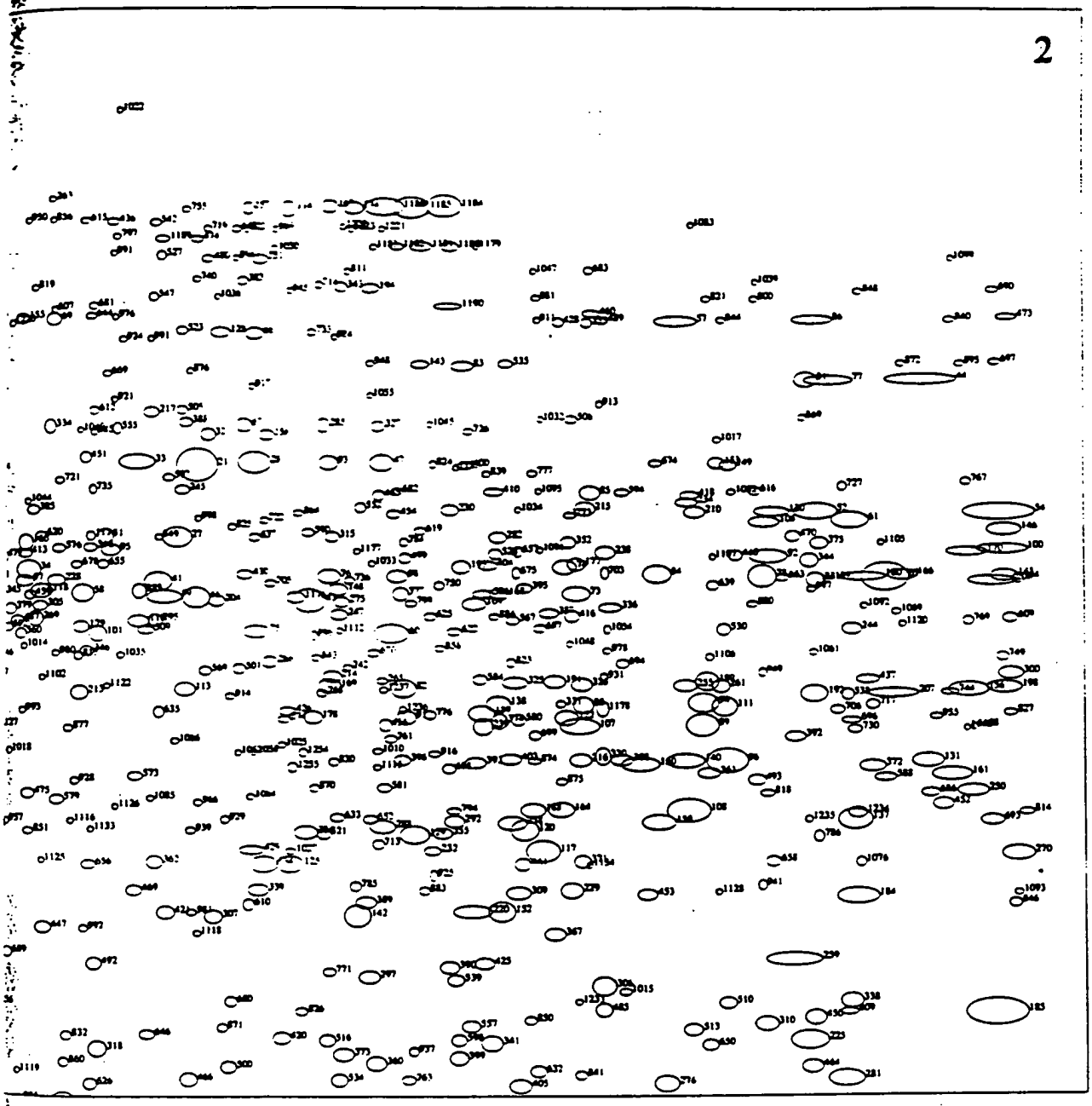

Figure 4. Upper right (high molecular weight, basic) quadrant (#2) of the rat liver map, showing spot numbers.

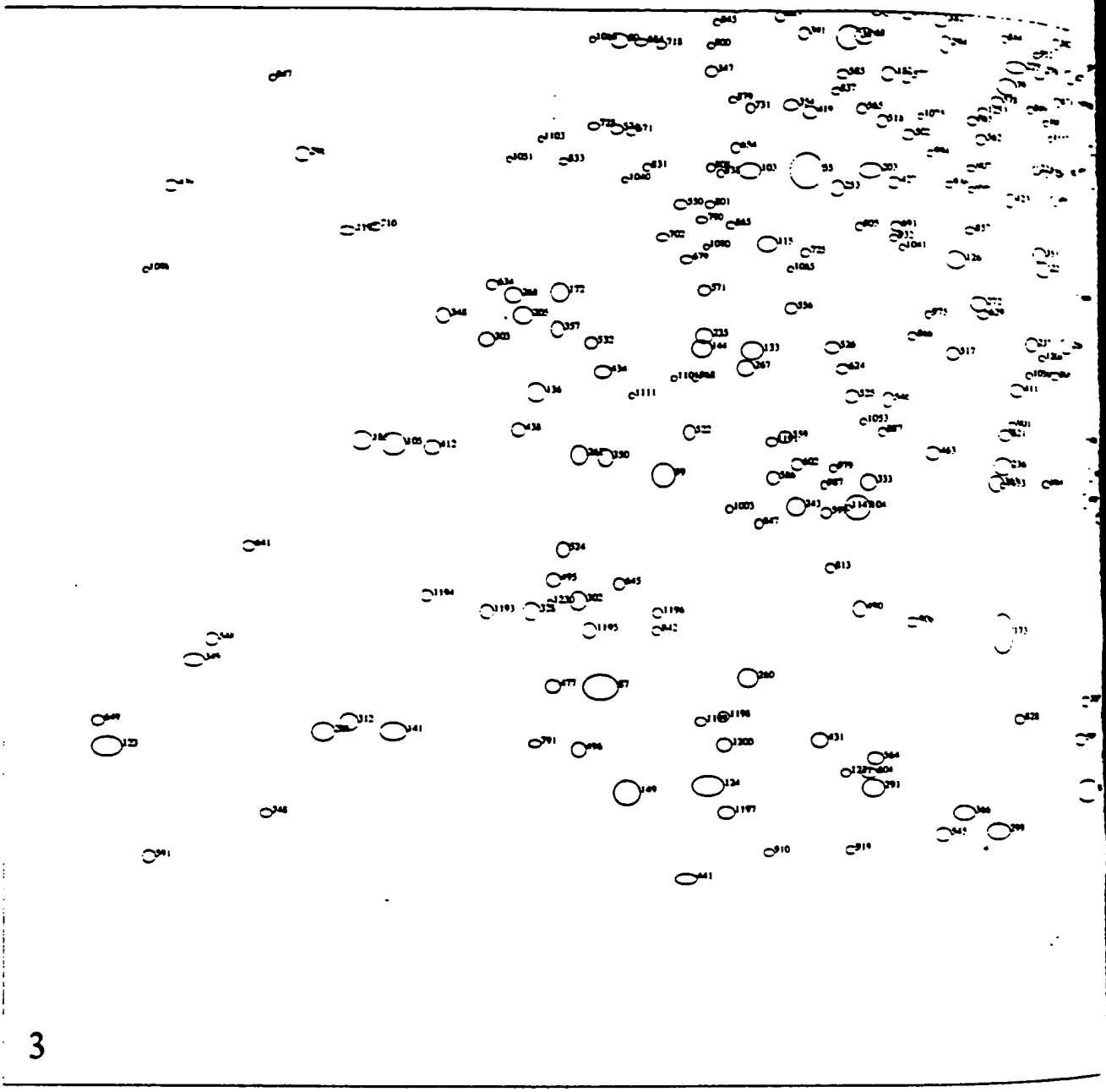

3

Figure 5. Lower left (low molecular weight, acidic) quadrant (#3) of the rat liver map, showing spot numbers.

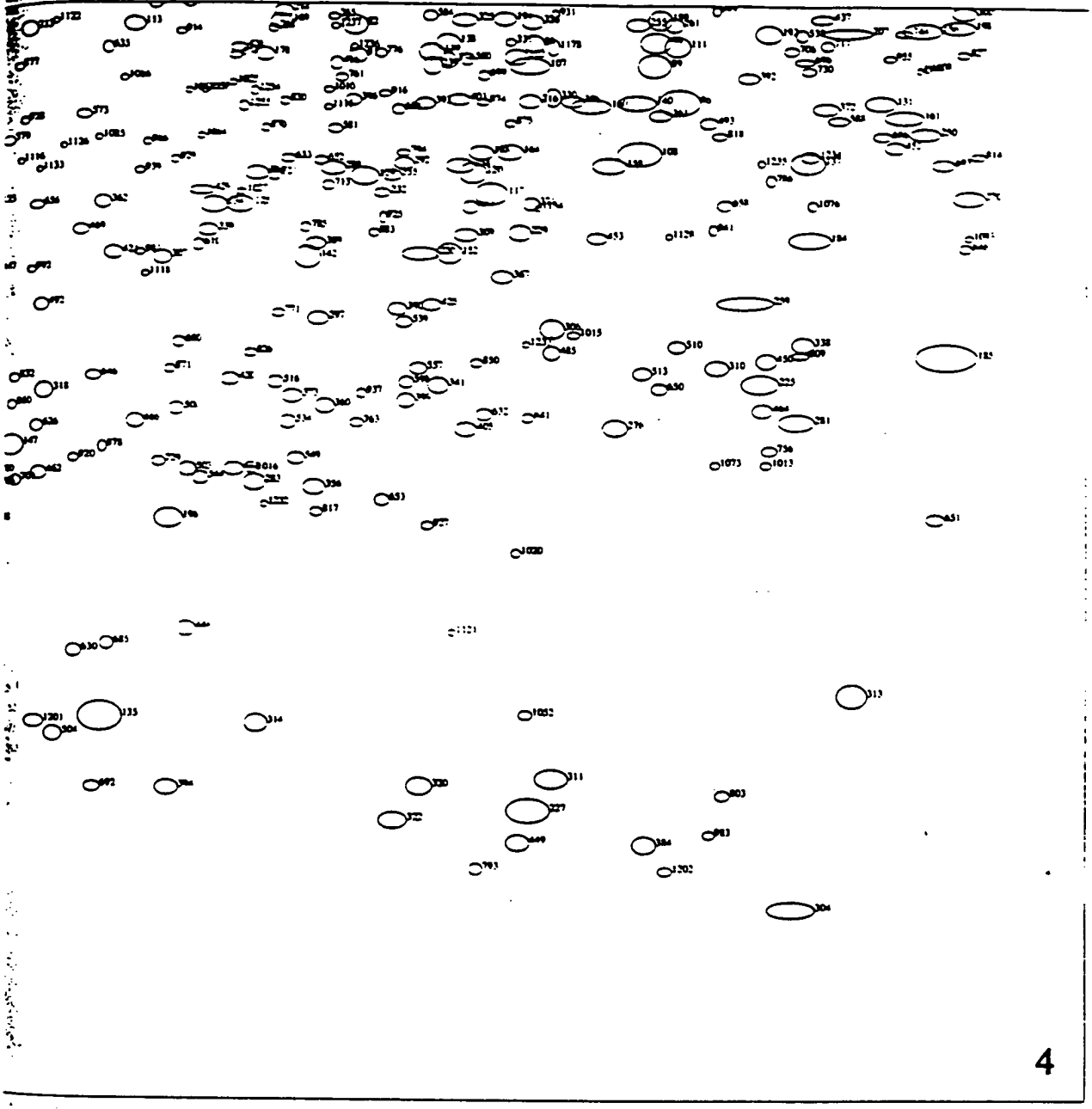

ure 6. Lower right (low molecular weight, basic) quadrant (#4) of the rat liver map, showing spot numbers.

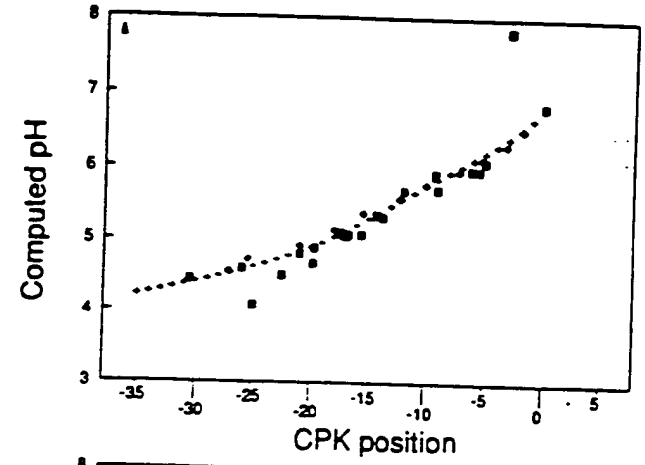

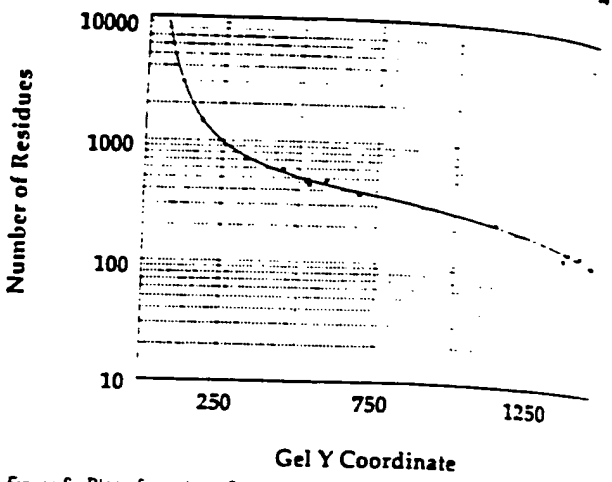

Figure 8. Plot of number of amino acids versus gel Y-position, with fitted curve used to predict molecular mass of unidentified proteins.

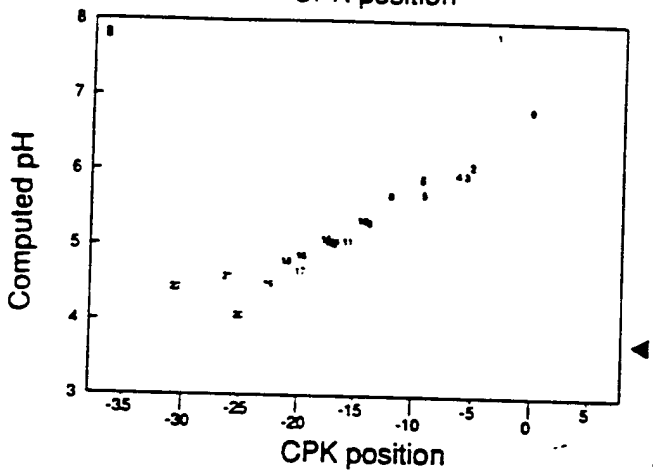

◀ *Figure 7.* (a) Plot of computed isoelectric point versus gel X-position for two sets of carbamylated standard proteins (rabbit muscle CPK [+] and human hemoglobin β chain, filled diamonds) and several other proteins (shaded squares). (b) The identities of the various proteins represented by the squares are indicated by the numbers in corresponding positions on (a); these refer to Table 4.

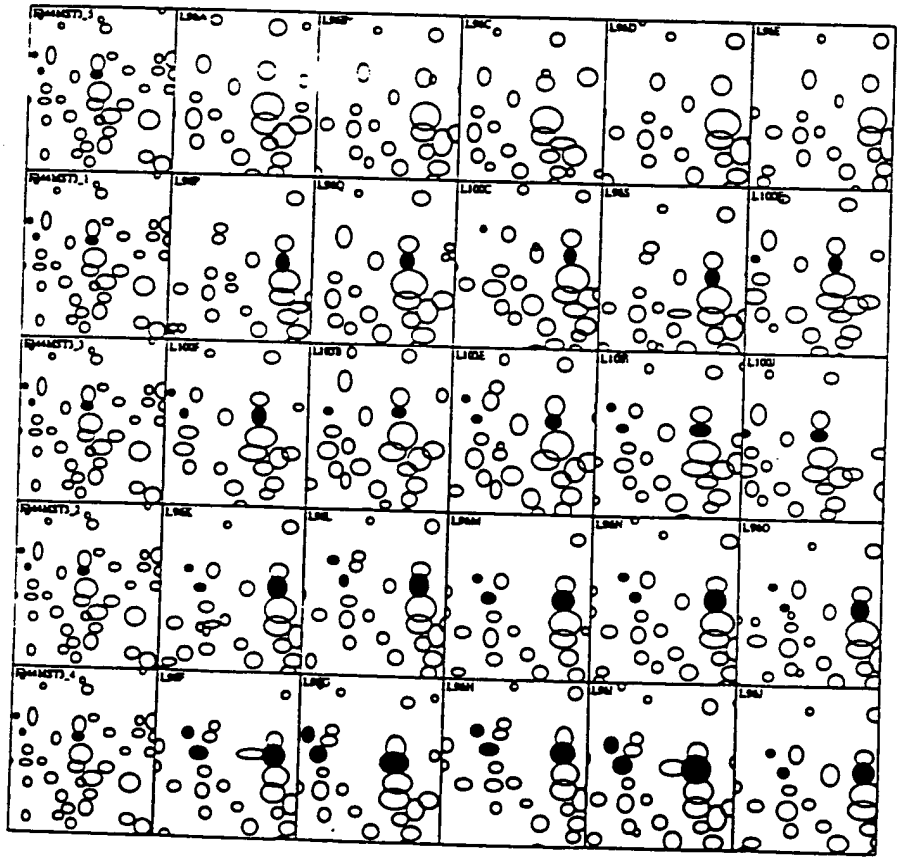

Figure 9. Montage showing effects in the region of MSN:413. The montage shows a small window into one portion of the 2-D pattern, one row of windows for each experimental group, and one panel for each gel in the experiment. The left-most pattern in each row is a group-specific copy of the master pattern followed by the patterns for the five individual rats in the group. The highlighted protein spots (filled circles) are spot 413 (on the right of each panel; identified as cytosolic HMG-CoA synthase) and two modified forms of it (1250 and 933). From the top, the rows (experimental groups) are: high cholesterol, controls, cholestyramine, lovastatin, and lovastatin plus cholestyramine.

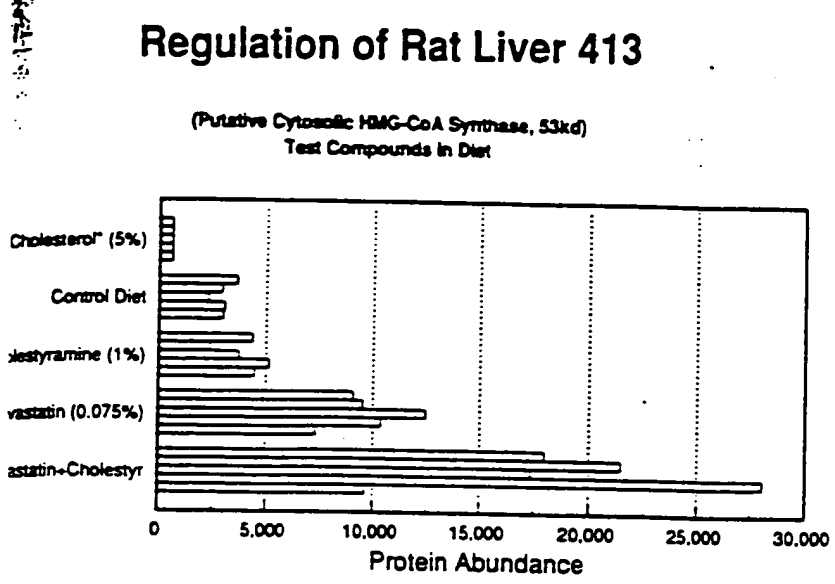

Figure 10. Bargraph showing the quantitative effects of various treatments on the abundance of MSN:413 (cytosolic HMG-CoA synthase) in the gels of Fig. 9.

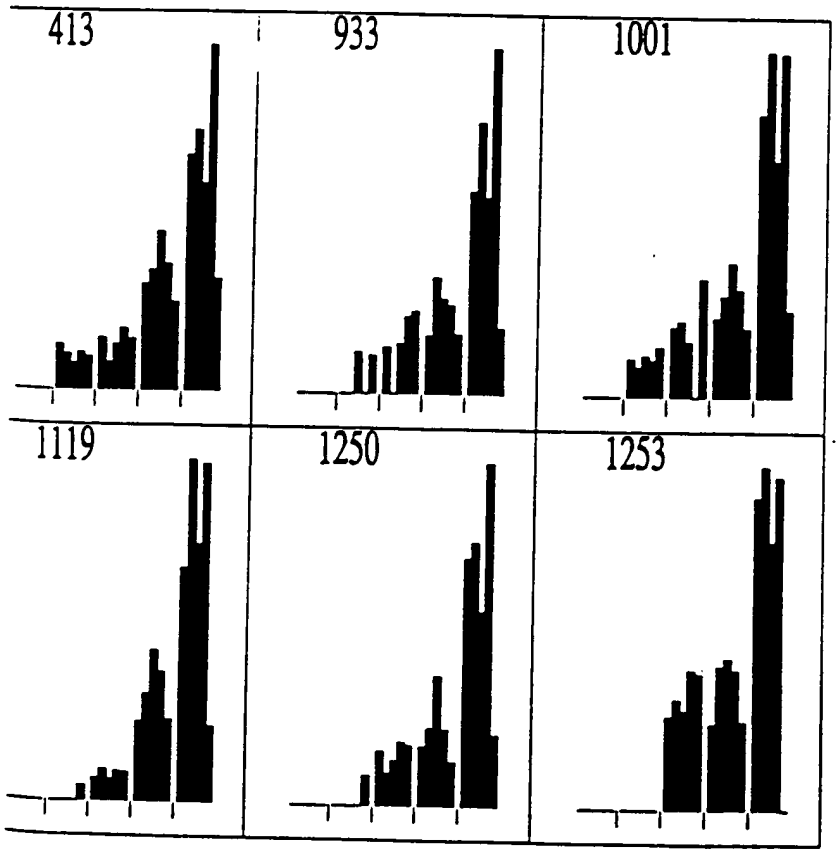

Figure 11. Bargraphs of a series of six coregulated spots including MSN:413. In the bargraphs, the abundances of the appropriate spot (master spot number shown at the top of the panel) in each animal are shown. The five five-animal groups are in the order (left to right): high cholesterol, controls, cholestyramine, lovastatin, and lovastatin plus cholestyramine. Each bar within a group represents one experimental animal liver (one 2-D gel). Note the correlated expression of the 6 spots, especially in the two far right (most strongly induced) groups.

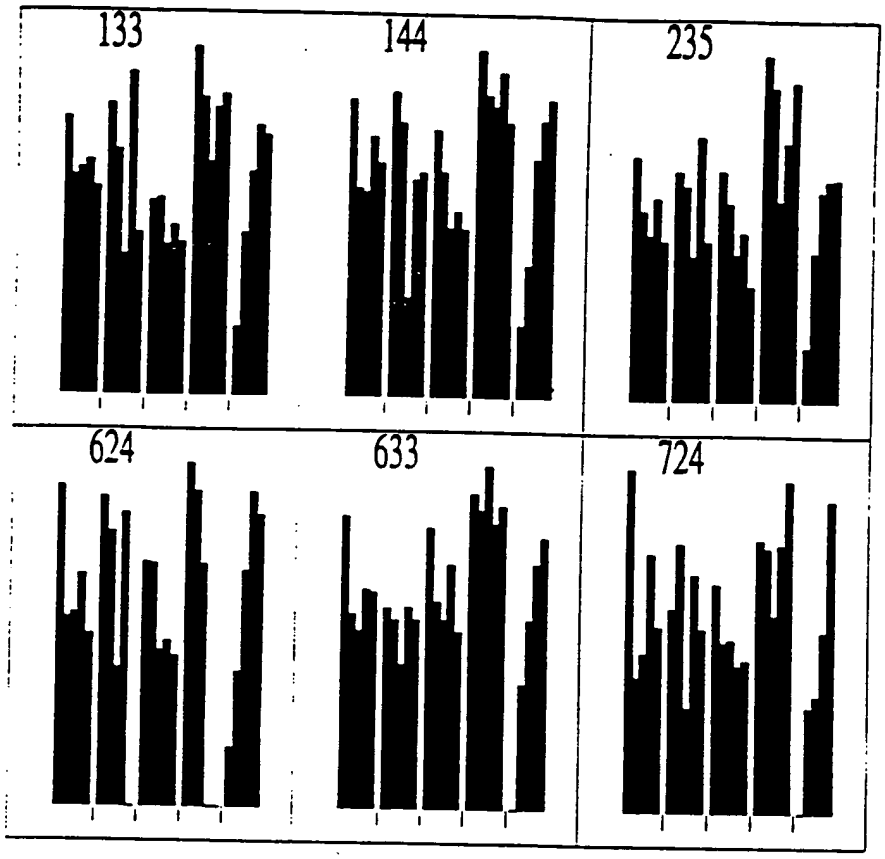

Figure 12. Data on a second coregulated group of spots, presented as in Fig. 11. The fourth experimental group (lovastatin) shows a modest induction, while the fifth group (lovastatin plus cholestyramine) does not.

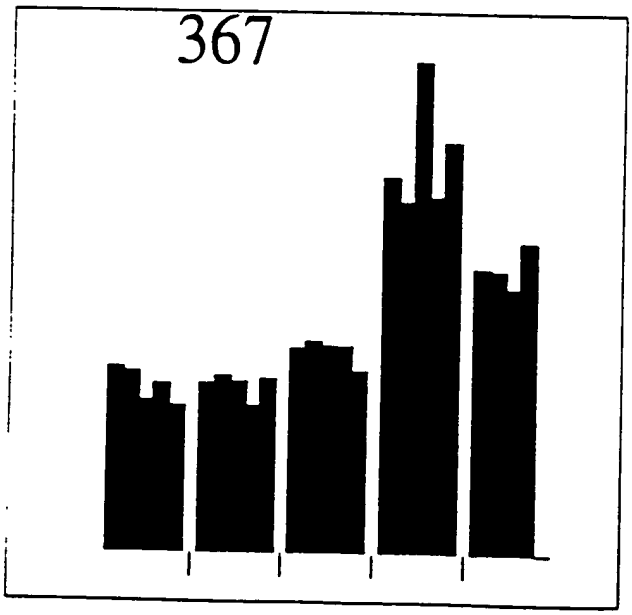

Figure 13. Data on spot MSN:367, presented as in Fig. 11. This protein shows unambiguously the anti-synergistic effect of lovastatin and cholestyramine (fifth group) as compared to lovastatin (fourth group). This response contrasts strongly with the regulation pattern seen in Fig. 11.

Addendum 2: Tables 1–4

Table 1. Master table of proteins in the rat liver database[a]

MSN	X	Y	CPKol	SDSMW	MSN	X	Y	CPKol	SDSMW	MSN	X	Y	CPKol	SDSMW
3	311	434	<-35.0	63,800	95	1119	536	-9.9	53,800	174	1364	183	-6.7	162,900
5	568	263	-24.3	102,900	96	1731	756	-2.0	40,700	175	825	393	-15.7	69,300
8	812	426	-16.0	64,800	97	1033	566	-11.4	51,600	177	1582	553	-3.6	52,600
11	549	268	-25.2	101,000	98	1406	565	-6.1	51,700	178	1321	710	-7.2	43,000
15	845	520	-15.3	55,200	99	578	1149	-23.8	25,000	179	1089	615	-10.4	48,300
17	629	589	-21.6	50,000	100	2004	538	>0.0	53,700	180	1866	567	-0.5	51,600
18	906	414	-14.0	66,300	101	1106	623	-10.1	47,900	181	411	295	-32.1	91,200
19	755	298	-17.5	90,200	102	482	455	-28.5	61,300	182	804	730	-16.2	42,000
20	649	403	-20.9	67,900	103	665	830	-20.2	37,300	184	1860	896	-0.6	34,500
21	1204	448	-8.7	62,100	104	773	1182	-17.0	23,800	185	1997	1017	>0.0	29,800
22	332	434	<-35.0	63,800	105	312	1117	<-35.0	26,100	186	279	1113	<-35.0	26,300
23	787	424	-16.6	65,000	106	1769	509	-1.5	56,100	187	773	296	-17.0	90,800
24	313	417	<-35.0	66,000	107	1585	720	-3.6	42,500	188	1538	807	-4.2	38,400
25	807	516	-16.1	55,500	108	1692	807	-2.4	38,300	191	1560	674	-3.9	44,900
27	1184	524	-9.0	54,900	109	1482	593	-4.8	49,700	192	1818	687	-0.9	44,200
28	1263	446	-8.0	62,400	110	778	516	-16.9	55,500	193	1469	556	-5.0	52,400
29	743	605	-17.8	49,000	111	1728	700	-2.0	43,500	194	1380	266	-6.4	101,600
30	768	112	-17.2	348,600	113	1191	680	-8.9	44,500	195	784	632	-16.7	47,300
32	1216	417	-8.6	66,000	114	1298	185	-7.5	160,800	196	1227	1185	-8.4	23,700
33	1145	445	-9.5	62,500	115	682	907	-19.6	34,100	197	667	553	-20.1	52,600
34	1037	555	-11.3	52,400	116	1146	610	-9.5	48,700	198	2006	681	>0.0	44,500
35	863	412	-14.9	66,600	117	1548	849	-4.1	36,500	199	1711	674	-2.2	44,900
36	712	606	-18.7	48,900	118	1050	577	-11.1	50,800	200	872	424	-14.7	65,000
38	763	694	-17.3	43,800	120	1530	828	-4.3	37,400	201	292	435	<-35.0	63,700
39	304	470	<-35.0	59,800	121	838	423	-15.4	65,200	202	736	253	-18.0	107,800
41	1165	569	-9.2	51,400	122	1572	712	-3.8	42,900	203	786	829	-16.7	37,400
42	684	607	-19.6	48,800	123	23	1433	<-35.0	15,300	204	1224	589	-8.5	50,000
43	1318	589	-7.3	50,000	124	621	1474	-21.9	13,900	205	439	983	-30.9	31,100
44	1924	362	-0.1	74,600	125	1298	862	-7.5	36,000	206	1994	571	>0.0	51,300
46	1203	586	-8.7	50,200	126	872	921	-14.7	33,500	207	1895	687	-0.3	44,200
47	1391	447	-6.3	62,300	127	1000	717	-12.0	42,600	208	240	1418	<-35.0	15,800
48	309	454	<-35.0	61,500	128	1229	311	-8.4	86,100	210	1700	499	-2.3	57,000
49	605	587	-22.5	50,100	129	1422	832	-5.8	37,300	211	902	517	-14.1	55,400
50	621	535	-21.8	53,900	130	1776	499	-1.4	57,000	213	1087	684	-10.4	44,400
51	1113	522	-10.0	55,000	131	1930	757	-0.1	40,700	214	1340	668	-7.0	45,200
52	1820	499	-0.9	57,000	132	660	537	-20.4	53,800	215	1591	495	-3.5	57,300
53	725	177	-18.3	170,800	133	666	1019	-20.2	29,700	216	1585	755	-3.6	40,700
54	2001	500	>0.0	56,900	134	1271	862	-7.9	36,000	217	1159	393	-9.3	69,300
55	722	830	-18.4	37,300	135	1161	1389	-9.3	16,800	218	931	572	-13.5	51,200
56	678	533	-19.8	54,100	136	453	1063	-29.7	28,100	219	713	177	-18.7	170,500
57	1682	302	-2.5	89,000	137	1858	823	-0.6	37,700	220	1479	911	-4.9	33,900
58	1091	580	-10.3	50,600	138	1504	697	-4.6	43,700	221	965	927	-12.8	33,300
59	1171	585	-9.2	50,300	139	1488	707	-4.8	43,200	223	934	716	-13.5	42,700
60	1400	624	-6.2	47,800	140	1689	756	-2.4	40,700	225	1812	1045	-1.0	28,800
61	1853	508	-0.6	56,200	141	311	1417	<-35.0	15,800	226	821	411	-15.8	66,800
62	1888	567	-0.4	51,500	142	1366	915	-6.7	33,800	227	1586	1483	-3.6	13,600
65	735	297	-18.1	90,500	143	1429	346	-5.7	77,900	228	1065	567	-10.8	51,600
66	1263	312	-8.0	85,900	144	615	1017	-22.1	29,800	229	1577	890	-3.7	34,800
67	1252	407	-8.1	67,300	145	2006	566	>0.0	51,600	230	1458	496	-5.2	57,300
68	779	692	-16.8	43,900	146	2006	518	>0.0	55,300	232	1440	849	-5.5	36,500
69	1064	296	-10.8	90,800	147	1070	1108	-10.7	26,500	234	1692	489	-2.4	57,900
71	656	589	-20.6	50,000	148	1347	578	-6.9	50,800	235	618	1004	-22.0	30,300
72	638	545	-21.2	53,100	149	541	1481	-25.7	13,700	236	920	1138	-13.7	25,400
73	1582	583	-3.6	50,400	150	1645	760	-2.8	40,500	237	952	1008	-13.1	30,200
74	1570	556	-3.8	52,300	151	1269	236	-7.9	117,000	238	1611	541	-3.2	53,500
75	1264	621	-8.0	48,000	152	1507	911	-4.5	33,900	239	1489	720	-4.8	42,500
76	1338	564	-7.0	51,800	153	1722	448	-2.1	62,100	240	501	448	-27.7	62,100
77	1833	363	-0.8	74,400	154	932	503	-13.5	56,600	241	1820	569	-0.9	51,400
78	1767	565	-1.5	51,700	155	1031	294	-11.4	91,400	242	1357	658	-6.8	45,800
79	925	738	-13.6	41,600	156	1970	684	>0.0	44,400	243	711	1182	-18.7	23,800
80	534	698	-26.1	43,600	157	1258	183	-8.1	162,400	244	1855	621	-0.6	48,000
81	1811	363	-1.0	74,500	158	1275	417	-7.8	65,900	245	1189	474	-8.9	59,300
82	1412	681	-6.0	44,500	159	1663	820	-2.6	37,800	246	551	459	-25.1	61,000
83	1471	347	-5.0	77,500	160	1034	527	-11.4	54,600	247	1348	604	-6.9	49,100
84	1662	563	-2.7	51,800	161	1953	771	>0.0	40,000	248	460	448	-29.3	62,100
85	1596	479	-3.4	58,900	162	1020	1482	-11.6	13,700	249	1733	451	-1.9	61,800
86	1817	301	-0.9	89,100	164	1566	806	-3.8	38,400	250	1974	788	>0.0	39,200
87	516	1371	-27.0	17,400	166	1905	565	-0.2	51,700	251	808	392	-16.1	69,500
88	1589	698	-3.5	43,600	167	1340	181	-7.0	164,900	252	874	553	-14.6	52,500
89	1706	719	-2.2	42,500	168	1506	583	-4.6	50,400	253	753	848	-17.6	36,500
90	651	329	-20.8	81,700	169	1338	678	-7.0	44,700	254	995	450	-12.1	61,900
91	1415	710	-6.0	43,000	170	1969	541	>0.0	53,500	255	1690	679	-2.4	44,600
92	1773	545	-1.4	53,200	171	800	378	-16.3	71,800	256	994	1006	-12.1	30,200
93	1338	446	-7.0	62,300	172	476	958	-28.7	32,100	257	508	464	-27.4	60,400
94	1708	696	-2.2	43,700	173	919	1314	-13.7	19,300	258	1517	820	-4.4	37,800

[a] Master table of proteins in the rat liver database, showing spot master number, gel position (*x* and *y*), isoelectric point relative to CPK standards, and predicted molecular mass (from the standard curve of Fig. 8).

MSN	X	Y	CPKol	SDSMW
259	1796	961	-1.1	31,900
260	661	1361	-20.4	17,700
261	1725	679	-2.0	44,600
262	496	1127	-28.0	25,800
263	1063	172	-10.9	177,400
265	1390	673	-6.3	45,000
266	510	437	-27.3	63,400
267	660	1038	-20.4	29,000
268	430	961	-31.0	31,900
269	1044	606	-11.2	48,900
270	2019	853	>0.0	36,300
271	857	422	-15.0	65,200
272	895	968	-14.2	31,700
274	1292	712	-7.6	42,900
275	1350	590	-6.9	49,900
276	1670	1089	-2.6	27,100
277	688	538	-19.4	53,700
278	961	718	-13.0	42,600
279	879	570	-14.5	51,300
281	1848	1084	-0.7	27,300
282	1505	525	-4.6	54,800
283	1313	1147	-7.3	25,100
284	1314	829	-7.3	37,400
285	1332	408	-7.1	67,200
286	1277	652	-7.8	46,100
288	1391	824	-6.3	37,600
289	1147	579	-9.5	50,700
290	925	511	-13.6	55,900
291	787	1476	-16.6	13,900
292	1462	818	-5.1	37,800
293	531	449	-26.3	62,000
294	860	698	-14.9	43,600
295	1162	609	-9.3	48,700
296	218	814	<-35.0	38,000
297	1377	979	-6.5	31,300
299	913	1523	-13.9	12,400
300	2012	667	>0.0	45,300
301	702	178	-19.0	169,200
302	494	1280	-28.1	20,400
303	403	1008	-32.6	30,100
304	1843	1585	-0.7	10,300
305	1049	593	-11.1	49,800
306	1608	989	-3.3	30,900
307	1219	916	-8.5	33,700
308	1627	755	-3.0	40,700
309	1524	892	-4.4	34,700
310	1769	1028	-1.5	29,400
311	1609	1451	-3.3	14,700
312	266	1408	<-35.0	16,100
313	1902	1365	-0.3	17,600
314	1316	1395	-7.3	16,600
315	1341	523	-7.0	54,900
318	1104	1053	-10.1	28,500
320	1480	1459	-4.9	14,400
321	850	603	-15.1	49,100
322	1454	1494	-5.3	13,300
323	670	626	-20.0	47,700
324	655	101	-20.6	420,500
325	1521	675	-4.4	44,800
326	1587	677	-3.6	44,700
327	1388	409	-6.3	67,000
328	448	1291	-30.0	20,100
330	1608	751	-3.3	40,900
331	1566	697	-3.8	43,700
332	531	471	-26.3	59,600
333	784	1156	-16.7	24,700
334	1059	407	-10.9	67,300
335	1593	303	-3.5	88,500
336	1616	598	-3.2	49,400
338	1854	1004	-0.6	30,300
339	1265	888	-8.0	34,900
340	581	585	-23.6	50,300
341	1497	1047	-4.7	28,700
343	1351	265	-6.8	102,200
344	1813	549	-0.9	52,800
345	1006	578	-11.9	50,800
346	1095	640	-10.3	46,800
347	625	728	-21.7	42,000
348	361	983	-35.3	31,100
349	110	1343	<-35.0	18,300
350	521	1130	-26.7	25,700
351	912	619	-13.9	48,100
352	1574	530	-3.7	54,300
353	981	912	-12.9	33,900
354	706	762	-18.9	40,400
355	1450	830	-5.3	37,300
356	1374	1152	-6.5	24,900
357	474	997	-28.7	30,600
358	798	346	-16.3	77,800
359	764	338	-17.3	79,400
360	1384	1068	-6.4	27,900
361	1713	769	-2.1	40,100
362	1161	859	-9.3	36,100
363	914	1156	-13.8	24,800
364	412	435	-32.0	63,700
365	741	486	-17.9	58,200
366	878	1503	-14.6	13,000
367	1560	935	-3.9	33,000
368	983	520	-12.4	55,200
369	434	441	-31.0	63,000
370	639	610	-21.2	48,700
371	1587	860	-3.6	36,100
372	1875	762	-0.5	40,400
373	1351	1059	-6.8	28,300
374	1506	715	-4.6	42,700
375	1823	532	-0.9	54,200
376	254	417	<-35.0	65,900
377	1409	583	-6.1	50,400
378	621	494	-21.8	57,500
379	1017	595	-11.7	49,600
381	953	598	-13.1	49,400
382	856	674	-15.0	44,900
383	1252	258	-8.1	105,300
384	1699	1518	-2.3	12,500
385	1042	493	-11.2	57,500
386	1490	583	-4.7	50,400
387	1554	603	-4.0	49,100
388	1193	404	-8.9	67,700
389	1374	902	-6.5	34,300
390	1456	969	-5.2	31,700
391	718	690	-18.5	44,000
392	1799	732	-1.1	41,900
393	1482	758	-4.8	40,600
394	1227	1461	-8.4	14,400
395	1530	577	-4.3	50,800
396	1410	755	-6.0	40,800
397	912	256	-13.9	106,400
399	1465	1063	-5.0	28,100
400	1473	450	-4.9	61,900
401	1029	1140	-11.5	25,300
403	1516	754	-4.4	40,800
404	1495	554	-4.7	52,500
405	1525	1092	-4.3	27,100
406	723	252	-18.4	108,000
409	650	663	-20.8	45,500
410	1501	478	-4.6	59,000
411	936	1057	-13.4	28,300
412	350	1120	-35.9	26,000
413	1033	538	-11.4	53,700
415	737	425	-18.0	64,900
416	1578	606	-3.7	48,900
417	646	496	-21.0	57,300
418	1695	482	-2.3	58,600
419	725	770	-18.3	40,000
420	1289	1041	-7.7	28,900
421	1171	912	-9.1	33,900
422	599	162	-22.8	193,700
423	929	856	-13.6	36,200
424	739	625	-17.9	47,700
425	1490	965	-4.7	31,800
426	1296	704	-7.6	43,200
427	810	843	-16.0	36,800
428	1565	303	-3.9	88,700
429	1259	847	-8.0	36,600
430	1253	562	-8.1	51,900
431	734	1426	-18.1	15,500
432	483	433	-28.5	63,900
434	518	1041	-26.9	28,900
435	1020	1170	-11.6	24,300
436	1122	196	-9.8	147,600
437	1870	673	-0.5	45,000
438	435	1102	-31.0	26,700
439	86	847	<-35.0	36,600
440	1740	544	-1.8	53,200
441	599	1571	-22.8	10,800
443	743	335	-17.8	80,100
446	801	668	-16.2	45,200
447	1050	926	-11.1	33,300
448	1245	1298	-8.2	19,800
449	1576	1516	-3.7	12,600
450	1818	1021	-0.9	29,600
451	1094	440	-10.3	63,100
452	1945	802	>0.0	38,600
453	1652	894	-2.8	34,600
454	1403	500	-6.1	56,900
456	1394	718	-6.3	42,600
457	905	436	-14.0	63,500
459	1038	581	-11.3	50,500
460	1598	294	-3.4	91,400
461	1528	863	-4.3	35,900
462	1098	1137	-10.2	25,400
463	849	1125	-15.2	25,800
464	1814	1072	-0.9	27,800
465	1388	481	-6.3	58,700
466	1194	1084	-8.9	27,300
468	577	467	-23.9	60,100
469	1140	888	-9.6	34,900
470	1797	524	-1.1	54,800
471	1293	1133	-7.6	25,500
472	618	655	-21.9	46,000
473	2009	299	>0.0	89,900
474	1205	215	-8.7	131,300
475	1035	788	-11.4	39,200
476	160	155	<-35.0	207,600
477	469	1370	-28.9	17,400
478	599	662	-22.8	45,600
479	1009	540	-11.8	53,500
480	1216	235	-8.6	117,400
482	816	346	-15.9	77,800
483	683	673	-19.3	44,900
485	1608	1013	-3.3	30,000
486	478	599	-28.6	49,300
487	1025	607	-11.5	48,800
488	1045	1186	-11.2	23,700
489	1609	301	-3.3	89,200
490	775	1289	-17.0	20,100
491	692	178	-19.3	169,300
492	1100	964	-10.2	31,800
493	1760	776	-1.6	39,700
494	882	247	-14.5	110,700
495	470	1258	-28.9	21,200
496	494	1436	-28.1	15,200
497	980	852	-12.5	36,400
499	1414	546	-6.0	53,100
500	1234	1072	-8.3	27,800
501	1246	659	-8.2	45,700
502	824	792	-15.7	39,000
503	1246	1134	-8.2	25,500
504	1115	1407	-9.9	16,200
505	1189	391	-8.9	69,700
506	1578	402	-3.7	68,000
507	787	250	-16.6	109,000
508	979	552	-12.5	52,800
509	1153	619	-9.4	48,100
510	1730	1006	-2.0	30,200

MSN	X	Y	CPKpI	SDSMW	MSN	X	Y	CPKpI	SDSMW	MSN	X	Y	CPKpI	SDSMW
511	809	484	-16.0	58,400	596	619	269	-21.9	100,500	674	1661	448	-2.7	62,100
512	1099	533	-10.2	54,100	597	1176	461	-9.1	60,700	675	1523	562	-4.4	51,900
513	1696	1034	-2.3	29,200	598	1465	1044	-5.0	28,800	676	708	642	-18.8	46,700
514	948	636	-13.2	47,100	599	741	1188	-17.9	23,600	677	919	615	-13.7	48,300
515	481	543	-28.5	53,400	600	907	402	-14.0	68,000	678	1085	551	-10.5	52,700
516	1334	1044	-7.1	28,800	601	687	658	-19.5	45,800	679	600	923	-22.7	33,400
517	868	1021	-14.8	29,700	602	712	1138	-18.7	25,400	680	1237	1004	-8.3	30,300
518	798	779	-16.3	39,600	603	898	181	-14.1	165,200	681	1103	283	-10.1	95,100
519	822	670	-15.7	45,100	604	783	1461	-16.7	14,400	682	1406	477	-6.1	59,100
520	632	165	-21.5	189,000	605	736	223	-18.0	125,300	683	1596	249	-3.4	109,800
521	1332	830	-7.1	37,300	606	629	273	-21.6	98,700	684	555	699	-24.8	43,500
522	603	1104	-22.6	26,600	607	1064	286	-10.8	94,000	685	1167	1313	-8.2	19,300
523	1190	309	-8.9	86,800	608	883	503	-14.5	56,700	686	1932	790	0.0	39,100
524	479	1226	-28.6	22,300	609	2012	610	>0.0	48,700	687	1545	619	-4.1	48,100
525	768	1066	-17.2	28,000	610	1255	903	-8.1	34,200	688	1456	764	-5.2	40,300
526	747	1016	-17.7	29,800	612	1103	391	-10.1	66,600	689	1011	953	-11.8	32,300
527	1170	231	-9.2	119,600	613	778	265	-16.9	102,000	690	1995	270	>0.0	100,200
528	1502	542	-4.6	53,400	614	824	518	-15.7	55,400	691	812	888	-16.0	34,900
530	1728	620	-2.0	48,000	615	1095	195	-10.3	149,100	692	1154	1461	-9.4	14,400
532	507	1011	-27.4	30,000	616	1759	478	-1.6	59,000	693	1993	819	>0.0	37,800
533	870	489	-14.7	57,900	617	994	372	-12.1	72,900	694	1628	656	-3.0	45,900
534	1347	1085	-6.9	27,300	618	751	374	-17.6	72,400	695	928	254	-13.6	107,000
535	1513	346	-4.5	77,800	619	1429	518	-5.7	55,300	696	1854	715	-0.6	42,700
536	308	654	<-35.0	46,000	620	1050	520	-11.1	55,200	697	1997	345	>0.0	78,000
538	1851	689	-0.7	44,100	621	923	1105	-13.7	26,600	698	957	563	-13.0	51,800
539	1463	982	-5.1	31,100	622	1462	622	-5.1	47,900	699	1540	730	-4.2	42,000
540	909	561	-13.9	52,000	623	759	225	-17.4	124,000	702	577	900	-23.8	34,400
541	625	289	-21.7	93,100	624	758	1038	-17.4	29,000	703	1610	562	-3.2	51,900
542	1164	198	-9.2	146,200	625	1438	606	-5.5	48,900	705	1278	571	-7.8	51,200
543	803	655	-16.2	45,900	626	1096	1089	-10.2	27,200	706	1841	704	-0.7	43,300
544	1259	1143	-8.0	25,200	627	942	548	-13.3	53,000	707	1018	1386	-11.7	16,900
545	856	1526	-15.0	12,200	628	809	621	-16.0	48,000	709	1074	1145	-10.7	25,100
546	803	1071	-16.2	27,800	629	899	979	-14.1	31,300	710	293	889	<-35.0	34,800
547	1162	274	-9.3	98,400	630	1135	1321	-9.6	19,100	712	720	412	-18.5	66,600
548	128	1321	<-35.0	19,000	631	979	615	-12.5	48,300	713	1386	841	-6.4	36,800
549	1355	1122	-6.8	25,900	632	1542	1076	-4.1	27,600	714	1328	263	-7.1	103,100
550	595	866	-23.0	35,800	633	1345	814	-6.9	38,000	715	698	433	-19.1	63,900
552	1369	494	-6.6	57,500	634	409	950	-32.2	32,400	716	701	481	-19.0	58,700
553	992	405	-12.2	67,600	635	1165	704	-9.2	43,300	717	1875	699	-0.5	43,600
555	1125	410	-9.8	66,900	636	774	604	-17.0	49,000	718	575	702	-23.9	43,400
556	705	975	-18.9	31,400	637	1263	524	-8.0	54,800	719	1216	204	-8.6	140,400
557	1477	1030	-4.9	29,300	638	952	411	-13.1	66,700	721	1069	464	-10.8	60,400
558	980	583	-12.5	50,400	639	1717	575	-2.1	51,000	722	1272	506	-7.9	56,400
559	700	1109	-19.1	26,400	640	994	292	-12.1	92,000	723	958	822	-13.0	37,700
560	1028	621	-11.5	48,000	641	165	1224	<-35.0	22,400	724	763	395	-17.3	69,100
562	898	794	-14.1	38,900	642	803	251	-16.2	108,900	725	720	916	-18.5	33,700
564	789	1446	-16.6	14,900	643	719	296	-18.5	90,700	726	1476	415	-4.9	66,200
565	777	766	-16.9	40,200	644	1100	294	-10.2	91,400	727	1846	473	-0.7	59,400
566	980	328	-12.5	81,900	645	534	1263	-26.1	21,000	728	510	783	-27.3	39,400
567	1519	611	-4.4	48,600	646	1153	1038	-9.4	29,000	729	1217	1126	-8.6	25,800
569	1212	661	-8.6	45,600	648	1246	204	-8.2	140,000	730	1858	724	-0.6	42,300
570	760	594	-17.4	49,700	649	14	1406	<-35.0	16,200	731	665	765	-20.2	40,300
571	618	956	-21.9	32,100	650	1713	1049	-2.1	28,600	733	1321	312	-7.2	85,900
573	1142	771	-9.6	40,000	651	1986	1183	>0.0	23,800	734	719	427	-18.5	64,600
574	532	787	-26.2	39,300	652	1378	816	-6.5	38,000	735	1101	473	-10.2	59,500
575	771	250	-17.1	109,200	653	1442	1165	-5.5	24,400	736	1359	569	-6.7	51,400
576	1068	534	-10.8	54,100	654	650	806	-20.8	38,400	738	696	220	-19.2	127,600
577	822	734	-15.7	41,800	655	1111	551	-10.0	52,700	739	687	409	-19.5	67,000
578	914	754	-13.8	40,800	656	1095	861	-10.3	36,000	740	1205	256	-8.7	106,200
579	1064	794	-10.8	38,900	657	1524	540	-4.4	53,600	741	995	563	-12.1	51,900
580	1524	714	-4.4	42,800	658	1777	860	-1.4	36,000	742	898	596	-14.1	49,500
581	1392	783	-6.3	39,400	659	391	584	-33.4	50,400	743	881	181	-14.5	165,900
582	982	686	-12.4	44,200	660	977	565	-12.5	51,700	744	1951	686	>0.0	44,200
584	1487	672	-4.8	45,000	661	658	166	-20.5	187,500	745	726	168	-18.3	183,600
585	758	731	-17.4	41,900	662	732	312	-18.1	86,100	746	999	643	-12.0	46,600
586	687	1152	-19.5	24,900	663	1787	567	-1.2	51,500	748	182	1503	<-35.0	13,000
587	930	523	-13.5	55,000	664	888	268	-14.4	100,900	749	2005	649	>0.0	46,300
588	1888	774	-0.4	39,900	665	889	775	-14.3	39,800	750	1448	575	-5.4	51,000
589	642	485	-21.1	58,300	666	715	221	-18.6	126,300	751	792	266	-16.5	101,900
590	1317	519	-7.3	55,300	667	781	227	-16.8	122,400	752	469	296	-28.9	90,600
591	65	1548	<-35.0	11,500	668	646	165	-21.0	189,100	754	664	254	-20.3	107,000
592	1014	614	-11.7	48,400	669	1116	353	-9.9	76,300	755	1195	184	-8.8	161,000
593	732	176	-18.1	172,300	670	1382	643	-6.4	46,600	756	1821	1113	-0.9	26,300
594	1627	478	-3.0	59,000	671	547	789	-25.3	39,200	757	909	246	-13.9	111,000
595	1009	1426	-11.8	15,500	673	984	746	-12.4	41,200	760	790	133	-16.5	264,900

MSN	X	Y	CPKpI	SDSMW
761	1399	733	-6.2	41,800
763	1416	1085	-5.9	27,300
764	2020	569	>0.0	51,400
765	651	475	-20.8	59,300
766	1052	1149	-11.1	25,000
767	1968	468	>0.0	59,900
768	1330	685	-7.1	44,300
769	1970	613	>0.0	48,500
770	857	617	-15.0	48,200
771	1337	974	-7.0	31,500
773	1576	502	-3.7	56,700
775	969	824	-12.8	37,600
776	1438	708	-5.5	43,100
777	1539	458	-4.2	61,000
778	850	434	-15.1	63,800
779	700	411	-19.1	66,800
780	1052	1136	-11.1	25,500
784	1413	529	-6.0	54,400
785	1364	885	-6.7	35,000
786	1822	835	-0.9	37,100
787	893	392	-14.3	69,500
790	616	882	-22.0	35,100
791	451	1429	-29.8	15,400
792	777	377	-16.9	72,000
793	1536	1543	-4.2	11,700
794	1461	807	-5.1	38,300
796	388	546	-33.6	53,100
797	1126	212	-9.8	133,700
798	933	437	-13.5	63,400
799	1420	593	-5.9	49,800
800	1756	279	-1.6	96,500
801	624	865	-21.7	35,800
802	898	547	-14.2	53,000
803	1775	1468	-1.4	14,200
804	573	196	-24.0	148,400
805	203	494	<-35.0	57,400
806	980	1039	-12.5	29,000
807	902	308	-14.1	87,200
808	625	827	-21.7	37,500
809	1851	1015	-0.7	29,900
810	440	573	-30.9	51,100
811	1358	249	-6.8	109,700
812	851	393	-15.1	69,400
813	745	1246	-17.8	21,600
814	2028	810	>0.0	38,200
815	1086	645	-10.4	46,500
816	629	313	-21.6	85,700
817	1376	1177	-6.5	24,000
818	1771	790	-1.4	39,100
819	1045	263	-11.2	103,100
820	984	362	-12.4	74,600
821	1712	279	-2.2	96,700
822	1256	205	-8.1	139,200
823	1517	654	-4.4	46,000
824	1442	449	-5.5	62,000
825	1240	513	-8.3	55,800
826	1309	1014	-7.4	29,900
827	2012	708	>0.0	43,100
828	937	1405	-13.4	16,200
830	1342	756	-7.0	40,700
831	562	826	-24.5	37,500
832	1073	1039	-10.7	29,000
833	481	820	-28.5	37,800
834	501	581	-27.8	50,500
837	751	748	-17.6	41,100
838	635	833	-21.3	37,200
839	1494	459	-4.7	60,900
840	1952	301	>0.0	89,300
841	1585	1080	-3.6	27,500
842	571	1312	-24.1	19,400
843	1325	649	-7.2	46,300
844	1727	301	-2.0	89,200
845	630	679	-21.5	44,600
846	2016	905	>0.0	34,200
847	673	1200	-19.9	23,200
848	1863	271	-0.6	99,500
849	1166	523	-9.2	54,900
850	1535	1024	-4.2	29,600
851	1035	826	-11.4	37,500
852	834	542	-15.5	53,400
855	499	220	-27.8	127,100
856	1063	194	-10.9	150,500
857	887	890	-14.4	34,800
858	1448	639	-5.4	46,900
859	706	311	-18.9	86,200
860	1070	1066	-10.7	28,000
861	472	347	-28.8	77,600
862	674	480	-19.9	58,800
864	1307	499	-7.4	57,000
865	645	887	-21.0	34,900
866	827	1004	-15.6	30,300
868	685	494	-19.5	57,400
869	1807	402	-1.0	68,000
870	1323	783	-7.2	39,400
871	1228	1031	-8.4	29,300
872	1904	346	-0.3	77,700
873	556	647	-24.8	46,400
874	1540	756	-4.2	40,700
875	1566	777	-3.8	39,700
876	1198	351	-6.8	76,800
877	1076	720	-10.6	42,500
878	1161	1111	-9.3	26,400
879	647	757	-20.9	40,700
880	1756	594	-1.6	49,700
881	1543	278	-4.1	97,100
883	1432	890	-5.7	34,800
884	922	689	-13.7	44,100
885	1103	414	-10.1	66,400
886	1501	607	-4.6	48,900
887	798	1103	-16.3	26,600
888	636	634	-21.3	47,200
889	951	759	-13.1	40,600
890	717	548	-18.6	52,900
891	1123	229	-9.8	121,200
892	891	413	-14.3	66,400
894	1245	234	-8.2	117,800
895	1962	346	>0.0	77,700
896	1322	626	-7.2	47,700
897	420	570	-31.4	51,300
898	662	428	-20.3	64,500
899	845	243	-15.3	113,000
900	624	703	-21.7	43,400
901	931	1094	-13.5	27,000
903	799	229	-16.3	121,000
904	765	520	-17.2	55,200
905	775	889	-17.0	34,800
907	888	824	-14.4	37,600
908	828	1303	-15.6	19,700
910	681	1544	-19.7	11,700
911	1544	301	-4.1	89,100
913	1606	387	-3.3	70,400
914	1237	688	-8.3	44,100
916	1442	749	-5.5	41,100
917	1260	367	-8.0	73,700
919	764	1541	-17.3	11,700
920	1133	1123	-9.7	25,900
921	1123	380	-9.8	71,500
923	829	242	-15.6	113,200
924	1131	318	-9.7	84,300
925	1441	874	-5.5	35,400
926	679	219	-19.7	128,200
927	1487	1191	-4.8	23,500
928	1082	775	-10.5	39,800
929	1231	816	-8.4	38,000
931	1609	670	-3.3	45,100
932	810	900	-16.0	34,400
933	965	520	-12.8	55,100
934	947	462	-13.2	60,600
936	865	843	-14.8	36,800
937	1421	1056	-5.9	28,400
939	1197	827	-8.8	37,500
941	1765	885	-1.5	35,000
942	602	472	-22.7	59,600
943	312	498	<-35.0	57,100
944	993	491	-12.1	57,700
945	1300	269	-7.5	100,300
946	630	423	-21.6	65,100
947	187	736	<-35.0	41,600
948	1380	344	-6.5	78,200
949	1766	665	-1.5	45,400
950	1038	193	-11.3	151,000
951	860	152	-14.9	213,000
952	957	701	-13.0	43,400
954	503	547	-27.6	53,000
955	1938	712	>0.0	42,900
957	1010	816	-11.8	37,900
959	768	174	-17.2	174,900
960	596	419	-23.0	65,700
961	557	409	-24.8	67,100
962	887	320	-14.4	83,900
963	564	334	-24.5	80,500
964	969	1155	-12.8	24,800
965	671	255	-20.0	106,600
966	1204	798	-8.7	38,700
967	910	154	-13.9	210,300
968	609	1048	-22.3	28,700
969	1285	206	-7.7	138,900
970	822	232	-15.8	119,300
971	976	437	-12.6	63,400
972	403	567	-32.6	51,600
974	279	495	<-35.0	57,400
975	844	981	-15.3	31,200
976	1124	295	-9.8	91,100
977	994	664	-12.1	45,400
978	1612	642	-3.2	46,700
979	749	1141	-17.7	25,300
980	1064	642	-10.8	46,700
981	1197	911	-8.8	33,900
983	1762	1508	-1.6	12,800
984	1344	317	-6.9	84,700
985	1024	1105	-11.5	26,600
987	739	1159	-17.9	24,600
988	816	555	-15.9	52,400
990	785	361	-16.7	74,900
991	1159	317	-9.3	84,500
992	1090	928	-10.4	33,300
993	1030	701	-11.5	43,400
994	847	811	-15.2	38,200
995	902	461	-14.1	60,700
996	888	847	-14.4	36,600
997	1815	579	-0.9	50,700
998	1205	504	-8.7	56,500
999	617	289	-22.0	93,100
1000	968	290	-12.8	92,700
1001	970	771	-12.7	40,000
1002	1736	478	-1.9	58,900
1003	643	1184	-21.1	23,700
1006	822	487	-15.8	58,100
1007	875	279	-14.6	96,400
1009	291	644	<-35.0	46,600
1010	1386	745	-6.4	41,200
1011	459	541	-29.4	53,500
1012	679	661	-19.7	45,600
1013	1818	1128	-0.9	25,800
1014	1032	634	-11.4	47,200
1015	1629	994	-3.0	30,700
1016	1311	1134	-7.4	25,500
1017	1722	424	-2.0	65,000
1018	1015	743	-11.7	41,300
1020	1574	1219	-3.7	22,500
1021	781	484	-16.8	58,400
1022	1129	83	-9.7	591,300
1023	812	317	-15.9	84,600
1024	785	446	-16.7	62,400
1025	1290	739	-7.7	41,500

N.	X
1	405
6	1296
7	856
8	1284
1	986
2	1547
3	1381
4	1525
5	1128
6	1226
9	1761
0	541
1	818
4	1036
5	1439
7	1540
8	1576
9	1089
0	949
1	426
2	1583
3	779
4	1613
5	1380
6	284
8	1261
0	393
1	1817
2	1245
4	1258
5	705
6	1181
7	529
8	508
9	1898
1	873
3	1768
5	836
6	1863
8	826
1	971
3	1697
5	1157
0	620
2	1867
3	2019
4	1546
5	1545
8	61
9	1954
1	588
2	1050
3	457
5	1884
6	1714
7	1717
8	1976
1	547
2	1348
5	1385
6	1078
7	975
8	1202
9	1022
0	1905
1	1512
2	1114
3	1464
5	1048
6	1122
8	1722
1	1098
3	1830
5	764
6	1968

MSN	X	Y	CPKoi	SDSMW
1026	405	552	-32.5	52,600
1027	1298	848	-7.5	36,500
1028	856	547	-15.0	53,000
1030	1284	226	-7.7	123,200
1031	986	822	-12.3	37,700
1032	1547	403	-4.1	67,900
1033	1381	551	-6.4	52,700
1034	1525	496	-4.3	57,200
1035	1128	645	-8.7	46,500
1036	1226	274	-8.5	98,300
1039	1761	262	-1.6	103,600
1040	541	839	-25.7	36,900
1041	818	910	-15.8	34,000
1044	1036	485	-11.3	58,300
1045	1439	407	-5.5	67,300
1047	1540	250	-4.2	109,200
1048	1576	635	-3.7	47,100
1049	1089	411	-10.4	66,700
1050	949	1040	-13.2	28,900
1051	426	818	-31.1	37,800
1052	1583	1385	-3.6	16,900
1053	779	1092	-16.8	27,000
1054	1613	620	-3.2	48,000
1055	1380	377	-6.5	72,000
1056	284	663	<-35.0	45,500
1058	1261	746	-8.0	41,200
1060	393	605	-33.3	49,000
1061	1817	645	-0.9	46,600
1062	1245	746	-8.2	41,200
1064	1258	792	-8.1	39,000
1065	705	934	-18.9	33,000
1066	1181	734	-9.0	41,800
1067	529	658	-26.3	45,800
1068	508	696	-27.4	43,700
1069	1898	604	-0.3	49,100
1071	873	609	-14.7	48,700
1073	1768	1128	-1.5	25,800
1075	836	773	-15.4	39,900
1076	1863	861	-0.6	36,000
1078	826	566	-15.7	51,600
1081	971	483	-12.7	58,500
1083	1697	202	-2.3	142,300
1085	1157	794	-9.4	38,900
1090	620	910	-21.9	34,000
1092	1867	597	-0.5	49,500
1093	2019	894	>0.0	34,600
1094	1546	538	-4.1	53,700
1095	1545	477	-4.1	59,100
1098	61	935	<-35.0	33,000
1099	1954	237	>0.0	116,000
1101	588	1048	-23.3	28,600
1102	1050	667	-11.1	45,200
1103	457	797	-29.5	38,800
105	1884	532	-0.4	54,200
1106	1714	649	-2.1	46,300
1107	1717	546	-2.1	53,100
1108	1976	722	>0.0	42,400
1111	547	1066	-25.3	28,000
1112	1348	621	-6.9	48,000
1115	1385	762	-6.4	40,400
116	1078	816	-10.6	38,000
1117	975	787	-12.6	39,300
1118	1202	933	-8.7	33,100
1119	1022	1076	-11.6	27,600
1120	1905	616	-0.3	48,300
1121	1512	1301	-4.5	19,700
1122	1114	677	-9.9	44,700
1123	1464	452	-5.1	61,700
1125	1048	857	-11.1	36,200
126	1122	802	-9.8	38,600
128	1722	892	-2.1	34,700
133	1098	825	-10.2	37,500
139	1830	569	-0.8	51,400
147	764	1182	-17.3	23,800
148	1968	724	>0.0	42,300
1153	921	1158	-13.7	24,700
1154	1594	864	-3.5	35,900
1161	637	400	-21.3	68,400
1162	623	397	-21.8	68,800
1163	665	397	-20.2	68,700
1168	564	528	-24.4	54,500
1170	552	529	-25.0	54,500
1171	538	524	-25.9	54,800
1172	545	514	-25.5	55,700
1174	1099	522	-10.2	55,000
1176	1304	586	-7.5	50,200
1177	1366	539	-6.6	53,700
1178	1608	702	-3.3	43,400
1179	1485	224	-4.8	124,900
1180	1459	224	-5.2	124,900
1181	1431	223	-5.7	125,100
1182	1407	223	-6.1	125,200
1183	1383	224	-6.4	124,700
1184	1454	182	-5.3	164,400
1185	1422	183	-5.8	162,600
1186	1394	182	-6.3	164,300
1189	1171	214	-9.2	131,800
1190	1457	286	-5.2	94,200
1191	686	1114	-19.5	26,200
1192	265	893	<-35.0	34,700
1193	403	1292	-32.6	20,000
1194	344	1275	<-35.0	20,600
1195	505	1311	-27.6	19,400
1196	572	1293	-24.1	20,000
1197	639	1502	-21.2	13,000
1198	637	1402	-21.3	16,300
1199	614	1407	-22.1	16,200
1200	637	1431	-21.3	15,400
1201	1095	1394	-10.3	16,600
1202	1719	1545	-2.1	11,600
1203	791	668	-16.5	45,200
1204	964	1021	-12.9	29,700
1205	313	195	<-35.0	148,700
1208	306	194	<-35.0	149,800
1209	320	197	<-35.0	147,400
1210	326	197	<-35.0	146,600
1211	394	294	-33.2	91,400
1212	402	294	-32.7	91,200
1214	386	294	-33.7	91,400
1215	641	329	-21.2	81,600
1216	660	329	-20.4	81,600
1217	914	266	-13.8	101,800
1218	873	245	-14.7	112,000
1219	970	372	-12.7	72,900
1220	1021	298	-11.6	90,100
1221	1392	205	-6.3	139,500
1222	1354	203	-6.8	141,800
1223	1362	205	-6.7	139,500
1224	673	540	-19.9	53,600
1225	614	542	-22.1	53,400
1226	603	539	-22.6	53,600
1227	696	623	-19.2	47,800
1228	707	628	-18.9	47,500
1229	475	447	-28.7	62,300
1230	466	1282	-29.0	20,400
1231	759	1461	-17.4	14,400
1232	1324	1170	-7.2	24,200
1233	1583	1005	-3.6	30,300
1234	1865	809	-0.6	38,200
1235	1812	817	-1.0	37,900
1236	1411	703	-6.0	43,400
1237	1392	682	-6.3	44,500
1238	794	410	-16.4	66,900
1239	769	407	-17.1	67,300
1240	740	406	-17.9	67,500
1241	743	511	-17.8	55,900
1242	713	510	-18.7	56,000
1243	682	509	-19.6	56,100
1244	663	504	-20.3	56,500
1245	565	582	-24.4	50,500
1246	547	577	-25.3	50,800
1247	530	576	-26.3	50,900
1249	516	572	-27.0	51,200
1250	973	536	-12.7	53,900
1251	607	532	-22.4	54,200
1252	665	529	-20.2	54,400
1253	899	766	-14.1	40,200
1254	1311	746	-7.4	41,200
1255	1300	761	-7.5	40,400
1257	1938	712	0.0	42,900
1258	1806	718	-1.0	42,600
1259	1727	715	-2.0	42,700
1260	1629	713	-3.0	42,800
1261	1555	717	-4.0	42,600
1262	1468	717	-5.0	42,600
1263	1413	722	-6.0	42,400
1264	1340	717	-7.0	42,600
1265	1263	717	-8.0	42,600
1266	1182	720	-9.0	42,500
1267	1110	717	-10.0	42,600
1268	1055	717	-11.0	42,600
1269	999	717	-12.0	42,600
1270	959	715	-13.0	42,700
1271	905	712	-14.0	42,900
1272	857	714	-15.0	42,800
1273	810	705	-16.0	43,300
1274	774	711	-17.0	42,900
1277	737	708	-18.0	43,100
1278	702	711	-19.0	42,900
1279	671	710	-20.0	43,000
1280	645	710	-21.0	43,000
1281	617	707	-22.0	43,100
1282	595	704	-23.0	43,300
1283	573	700	-24.0	43,500
1284	552	695	-25.0	43,700
1285	536	694	-26.0	43,800
1286	515	687	-27.0	44,200
1287	496	683	-28.0	44,400
1288	467	669	-29.0	45,200
1289	447	667	-30.9	45,300
1290	427	655	-31.0	45,900
1291	412	655	-32.0	45,900
1292	397	652	-33.0	46,100
1293	381	654	-34.0	46,000
1294	365	653	-35.0	46,100
1295	348	653	<-35.0	46,100

Table 2. Table of some identified proteins

POP name	Protein name	MSN's	Basis for identification
IDS:3_ALPHA_HDDH	3-α-hydroxysteroid-dihydrodiol-dehydrogenase, an enzyme of steroid metabolism	137, 159	Pure protein and antibody provided by Dr. T.M. Penning, Department of Pharmacology, School of Medicine, University of Pennsylvania.
IDS:ACTIN_BETA	β cellular actin, a cytoskeletal protein	38	Homologous position with respect to other mammalian systems
IDS:ACTIN_GAMMA	γ cellular actin, a cytoskeletal protein	68	Homologous position with respect to other mammalian systems
IDS:ALBUMIN	Serum albumin, mature form.	21, 28, 33	Predominance in rat plasma
IDS:APO_A-I	Apo A-I plasma lipoprotein, mature form (tentative).	236, 463	Presence in rat plasma, regulation by some lipid-lowering drugs
IDS:CALMODULIN	Calmodulin, an acidic cytosolic calcium-binding protein	123, 649	Homologous position with respect to other mammalian systems
IDS:CATALASE	Catalase (peroxisomal)	54, 61, 106	Presence in purified peroxisomes, similarity in position to mouse catalase
IDS:CPKSPOTS	Spots contributed by the CPK charge standards (not rat liver proteins)	1257 - 1295	
IDS:CPS	Carbamoyl phosphate synthase	114, 157, 167, 174, 1184, 1185, 1186, 1222	Pure protein provided by Dr. Margaret Marshall, Department of Pharmacology, Medical School, University of Wisconsin - Madison.
IDS:CYTOCHROME_B5	Cytochrome b5	87, 477	Pure protein provided by Dr. Andrew Parkinson, Department of Pharmacology, Toxicology and Therapeutics, University of Kansas Medical Center
IDS:FABP-L	Liver fatty-acid binding protein	227	Pure protein provided by Dr. Nathan Bass, Department of Medicine, University of California School of Medicine, San Francisco
IDS:HMG-COA_SYNTHASE	Cytosolic HMG-CoA Synthase	133, 144, 235, 413	Antibody provided by Dr. Michael Greenspan, Merck Sharp & Dohme Research Laboratories, Rahway, NJ
IDS:LAMIN_B	Lamin B, a nuclear protein	415, 734	Homologous position with respect to other mammalian systems
IDS:MITCON:1	Mitcon:1 (F1 ATPase β subunit), a mitochondrial inner membrane	17, 49, 71, 340, 1245, 1246, 1247, 1249	Homologous position with respect to other mammalian systems, presence in mitochondria
IDS:MITCON:2	Mitcon:2, a mitochondrial matrix stress protein equivalent to E.	15, 25, 110, 1241, 1242, 1243, 1244	Homologous position with respect to other mammalian systems, presence in mitochondria
IDS:MITCON:3	Mitcon:3, a mitochondrial matrix stress protein, likely analog of	18, 35, 226, 600, 1238, 1239, 1240	Homologous position with respect to other mammalian systems, presence in mitochondria
IDS:NADPH_P450_RED	NADPH cytochrome P-450 reductase, frequently co-induced with P-450's	175, 251, 812	Pure protein provided by Dr. Andrew Parkinson, Department of Pharmacology, Toxicology and Therapeutics, University of Kansas Medical Center
IDS:PDI	Protein disulphide isomerase 1	168, 1170, 1171, 1172	Sequence information obtained by R.M. Van Frank, Lilly Research Laboratories, Indianapolis
IDS:PLASMA_PROTEINS	Rat plasma proteins observed in liver	21, 28, 33, 44, 72, 102, 115, 197, 236, 246, 248, 257, 293, 332, 347, 364, 369, 419, 432, 463, 468, 518, 562, 605, 623, 666, 667, 725, 738, 790, 865, 903, 926	Plasma coelectrophoresis studies
IDS:PRO-ALBUMIN	Serum albumin precursor	47, 93	Relative position to mature albumin, presence in microsomes
IDS:PYRCARBOX	Pyruvate carboxylase	179, 1180, 1181, 1182, 1183	Pavlica, R.J., et al., BBA (1990) *1022* 115-125.
IDS:SOD	Superoxide dismutase	135	Sequence information obtained by R.M. Van Frank, Lilly Research Laboratories, Indianapolis
IDS:TUBULIN_ALPHA	α tubulin, a cytoskeletal protein	56, 132, 1224, 1252	Homologous position with respect to other mammalian systems
IDS:TUBULIN_BETA	β tubulin, a cytoskeletal protein	50, 1225, 1226, 1251	Homologous position with respect to other mammalian systems

e 3. Computed pI's of two sets of carbamylated protein standards: Rabbit muscle CPK and human hemoglobin (Hb)

Protein Name	PIR Name	#ASP 3.9	#GLU 4.1	#HIS 6.0	#LYS 10.8	#ARG 12.5	NH2- 7.0	Calc pI	Real CPK
Rabbit muscle CPK	KIRBCM	28	27	17	34	18	1	6.84	0.0
		28	27	17	33	18	1	6.67	-1
		28	27	17	32	18	1	6.54	-2
		28	27	17	31	18	1	6.42	-3
		28	27	17	30	18	1	6.31	-4
		28	27	17	29	18	1	6.21	-5
		28	27	17	28	18	1	6.12	-6
		28	27	17	27	18	1	6.03	-7
		28	27	17	26	18	1	5.94	-8
		28	27	17	25	18	1	5.85	-9
		28	27	17	24	18	1	5.76	-10
		28	27	17	23	18	1	5.67	-11
		28	27	17	22	18	1	5.58	-12
		28	27	17	21	18	1	5.48	-13
		28	27	17	20	18	1	5.39	-14
		28	27	17	19	18	1	5.29	-15
		28	27	17	18	18	1	5.20	-16
		28	27	17	17	18	1	5.12	-17
		28	27	17	16	18	1	5.04	-18
		28	27	17	15	18	1	4.96	-19
		28	27	17	14	18	1	4.89	-20
		28	27	17	13	18	1	4.83	-21
		28	27	17	12	18	1	4.77	-22
		28	27	17	11	18	1	4.71	-23
		28	27	17	10	18	1	4.66	-24
		28	27	17	9	18	1	4.61	-25
		28	27	17	8	18	1	4.56	-26
		28	27	17	7	18	1	4.52	-27
		28	27	17	6	18	1	4.48	-28
		28	27	17	5	18	1	4.44	-29
		28	27	17	4	18	1	4.40	-30
		28	27	17	3	18	1	4.36	-31
		28	27	17	2	18	1	4.32	-32
		28	27	17	1	18	1	4.29	-33
		28	27	17	0	18	1	4.25	-34
		28	27	17	0	18	0	4.22	-35
Hb-beta, human	HBHU	7	8	9	11	3	1	7.18	
		7	8	9	10	3	1	6.79	
		7	8	9	9	3	1	6.53	-1.8
		7	8	9	8	3	1	6.32	-3.2
		7	8	9	7	3	1	6.13	-5.3
		7	8	9	6	3	1	5.96	-7.2
		7	8	9	5	3	1	5.78	-10.0
		7	8	9	4	3	1	5.59	-12.3
		7	8	9	3	3	1	5.37	-15.5
		7	8	9	2	3	1	5.14	-18.0
		7	8	9	1	3	1	4.91	-21.0
		7	8	9	0	3	1	4.71	-25.5
		7	8	9	0	3	0	4.54	-27.2

Table 4. Computed pI's of some known proteins related to measured CPK pI's

	Protein Name	PIR Name	#ASP 3.9	#GLU 4.1	#HIS 6.0	#LYS 10.8	#ARG 12.5	Calc pI	Real CPK
0	Creatine phospho kinase (CPK), rabbit muscle	KIRBCM	28	27	17	34	18	6.84	0.0
1	Fatty acid-binding protein, rat hepatic	FZRTL	5	13	2	16	2	7.83	-3.0
2	b2-microglobulin, human	MGHUB2	7	8	4	8	5	6.09	-5.0
3	Carbamoyl-phosphate synthase, rat	SYRTCA	72	96	28	95	56	5.97	-5.5
4	Proalbumin (serum albumin precursor), rat	ABRTS	32	57	15	53	27	5.98	-6.2
5	Serum albumin, rat	ABRTS	32	57	15	53	24	5.71	-9.0
6	Superoxid dismutase (Cu-Zn, SOD), rat	A26810	8	11	10	9	4	5.91	-9.2
7	Phospholipase C, phophoinositide-specific (?), rat	A28807	34	42	9	49	21	5.92	-9.2
8	Albumin, human	ABHUS	36	61	16	60	24	5.70	-11.9
9	Apo A-I lipoprotein, rat	A24700	18	24	6	23	12	5.32	-13.7
10	proApo A-I lipoprotein, human	LPHUA1	16	30	6	21	17	5.35	-14.3
11	NADPH cytochrome P-450 reductase, rat	RDRTO4	41	60	21	38	36	5.07	-15.6
12	Retinol binding protein, human	VAHU	18	10	2	10	14	5.04	-16.9
13	Actin beta, rat	ATRTC	23	26	9	19	18	5.06	-17.2
14	Actin gamma, rat	ATRTC	20	29	9	19	18	5.07	-16.8
15	Apo A-I lipoprotein, human	LPHUA1	16	30	5	21	16	5.10	-17.5
16	Apo A-IV lipoprotein, human	LPHUA4	20	49	8	28	24	4.88	-19.7
17	Tubulin alpha, rat	UBRTA	27	37	13	19	21	4.66	-19.8
18	F1ATPase beta, bovine	PWBOB	25	36	9	22	22	4.80	-21.0
19	Tubulin beta, pig	UBPGB	26	36	10	15	22	4.49	-22.5
20	Protein disulphide isomerase (PDI), rat hepatic	ISRTSS	43	51	11	51	9	4.07	-25.0
21	Cytochrome b5, rat	CBRT5	10	15	6	10	4	4.59	-26.0
22	Apo C-II lipoprotein, human	LPHUC2	4	7	0	6	1	4.44	-30.5
	Amino acid pI assumed in calulation:		3.9	4.1	6.0	10.8	12.5		

N. Leigh Anderson[1]
Ricardo Esquer-Blasco[1]
Jean-Paul Hofmann[1]
Lydie Meheus[2]
Jos Raymackers[2]
Sandra Steiner[3]
Frank Witzmann[4]
Norman G. Anderson[1]

[1]Large Scale Biology Corporation, Rockville, MD
[2]Innogenetics NV, Ghent
[3]Sandoz Pharma Ltd, Drug Safety Assessment, Toxicology, Basel
[4]Molecular Anatomy Laboratory, Indiana University Purdue University Columbus, Columbus, IN

An updated two-dimensional gel database of rat liver proteins useful in gene regulation and drug effect studies

We have improved upon the reference two-dimensional (2-D) electrophoretic map of rat liver proteins originally published in 1991 (N. L. Anderson *et al.*, *Electrophoresis* 1991, *12*, 907–930). A total of 53 proteins (102 spots) are now identified, many by microsequencing. In most cases, spots cut from wet, Coomassie Blue stained 2-D gels were submitted to internal tryptic digestion [2], and individual peptides, separated by high-performance liquid chromatography (HPLC), were sequenced using a Perkin-Elmer 477A sequenator. Additional spots were identified using specific antibodies.

Figure 1 shows the current annotated 2-D map of F344 rat liver, analyzed using the Iso-DALT system (20 × 25 cm gels) and BDH 4–8 carrier ampholytes. Both the map itself and the master spot number system remain the same as shown in the original publication. Table 1 lists the important features of each identification shown, including the gel position, p*I*, and M_r for the most abundant or most basic form of each protein. Using this extended base of identified spots, a series of four improved calibration functions has been derived for the p*I* and SDS-M_r axes (the first two of which are shown in Fig. 2A and B). Both forward and reverse functions are derived, so that one can compute the physical properties of a spot with a given gel location, or inversely compute the gel position expected for a protein having given physical properties:

$$Y_{\text{RATLIVER}} = f_{M_r\text{–RATLIVER Y}}(M_{r,\text{SEQUENCE-DERIVED}}) \quad (1)$$

$$X_{\text{RATLIVER}} = f_{\text{pI–RATLIVER X}}(\text{p}I_{\text{SEQUENCE-DERIVED}}) \quad (2)$$

$$M_{r,\text{GEL-DERIVED}} = f_{\text{RATLIVER Y–}M_r}(Y_{\text{RATLIVER}}) \quad (3)$$

$$\text{p}I_{\text{GEL-DERIVED}} = f_{\text{RATLIVER X–pI}}(X_{\text{RATLIVER}}) \quad (4)$$

A spreadsheet program (in Microsoft Excel) was developed to facilitate flexible computation of p*I*'s from amino acid sequence data, and the results were entered into a relational database (Microsoft Access). A table of spot positions and sequence-derived pI's and M_r's was fitted with a large series of analytic equations using Tablecurve (Jandel Scientific), and the four conversion Eqs. (1)–(4), relating computed p*I* and gel *X* coordinate, or computed molecular weight and gel *Y* coordinate, were selected, based on criteria of simplicity, goodness of fit and favorable asymptotic behavior. Table 2 lists the equations and coefficients. Application of Eqs. (3) and (4) to a spot's *X* and *Y* coordinates, given in [1], produce improved M_r estimates, and allow computation of p*I* directly in pH units, instead of in terms of positions relative to creatine phosphokinase (CPK) charge standards. The inverse Eqs. (1) and (2) were used to compute the gel positions of a series of p*I* and M_r tick marks. These tick marks were plotted with SigmaPlot (Jandel), together with fiducial marks locating several prominent spots, and the resulting graphic was aligned over the synthetic gel image (computed by Kepler from the master gel pattern) using Freelance (Lotus Development). Maps were printed as Postscript output from Freelance, either in black and white (as shown here) or in color, where label color indicates subcellular location (available from the first author upon request). We have also used the rat liver 2-D pattern as presented here to calibrate the patterns of other samples. Using mixtures of rat liver and mouse liver samples, for example, we made composite 2-D patterns that allow use of the rat pattern to standardize both axes of the mouse pattern. This was accomplished by deriving transformations relating the rat and mouse *X*, and separately the rat and mouse *Y*, axes (Table 2, lower half; Fig. 2C and D) based on a series of spots that coelectrophorese in these closely related species. These functions were then applied to derive equations relating the mouse liver *X* and *Y* to p*I* and SDS-M_r (Eqs. 5 and 6 below). The resulting standardized 2-D pattern for B6C3F1 mouse liver is shown in Fig. 3.

$$M_{r,\text{MOUSELIVER}} = f_{\text{RATLIVER Y–}M_r}(U_{\text{MOUSELIVER Y–RATLIVER Y}}(Y_{\text{MOUSELIVER}})) \quad (5)$$

$$\text{p}I_{\text{MOUSELIVER}} = f_{\text{RATLIVER X–pI}}(U_{\text{MOUSELIVER X–RATLIVER X}}(X_{\text{MOUSE LIVER}})) \quad (6)$$

A slightly more complex approach can be used to standardize samples that have few or no spots co-electrophoresing with rat liver proteins. In this case, a 2-D gel is prepared with a mixture of the two samples, and four functions (forward and backward, each for *X* and *Y*) are derived relating each sample's own master pattern to the composite. The required functions are then applied in a nested fashion to yield the desired result (using rat plasma as an example):

$$M_{r,\text{RATPLASMA}} = f_{\text{RATLIVER Y–}M_r}(U_{\text{RATPLASMA+LIVER Y–RATLIVER Y}}(U_{\text{RATPLASMA Y–RATPLASMA+LIVER Y}}(Y_{\text{RATPLASMA}}))) \quad (7)$$

Correspondence: Dr. Leigh Anderson, Large Scale Biology Corporation, 9620 Medical Center Drive, Rockville, MD 20850-3338 USA (Tel: +301-424-5989; Fax: +301-762-4892; email: leigh@lsbc.com)

Keywords: Two-dimensional polyacrylamide gel electrophoresis / Liver / Map / Identification / Calibration

0173-0835/95/1010-1977 $5.00+.25/0

Table 1. continued

MSN[a]	Protein IDb)	Protein name	Identification comments	Gel X[c]	Experimental pI[d]	Gel Y[c]	Experimental M_r[d]
1184, 1186, 114, 174, 118 5, 167, 157	CPSM_RAT	Carbamyl phosphate synthase	2-D of pure protein; comfirmed by *N*-terminal sequence and AAA	1453.56	6.05	181.64	160 640
54, 61	CATA_RAT	Catalase	Internal sequence	2000.81	6.73	499.64	58 968
136	COX2_RAT	COX-II	Ab (J. W. Taanman), confirmed by internal sequence	452.57	4.61	1062.67	25 504
87	CYB5_RAT	Cytochrome B5	2-D of pure protein; Ab; confirmed by AAA	515.68	4.73	1370.55	18 493
41	CK-RAT[e]	Cytokeratin	Location in cytoskeletal fraction	1165.12	5.75	569.09	51 448
29	CK-RAT[e]	Cytokeratin	Location in cytoskeletal fraction	743.11	5.15	605.23	48 187
5, 11	ENPL-RAT[e]	Endoplasmin	Ab (F. Witzmann)	567.73	4.83	263.37	112 194
60	ENOA_RAT	Enolase A	Internal sequence and AAA	1399.78	6.00	623.54	46 674
27	ER60_RAT	ER-60	*N*-Terminal sequence (R. M. Van Frank)	1184.20	5.77	523.51	56.169
17	ATPB_RAT	F1 ATPase β	*N*-Terminal sequence and AAA	629.06	4.95	588.83	49 620
196	ATP7_RAT	F1 ATPase δ	Internal sequence	1227.24	5.82	1184.65	22 310
79	F16P_RAT	Fructose-1.6-bis-phosphatase	Uncertain; by comparison with ID in Garrison and Wager (JBC 257:13135-13143)	924.54	5.44	737.77	38 858
62, 78	DHE3_RAT	Glutamate dehydrogenase	*N*-Terminal sequence and internal sequence	1887.39	6.55	566.92	51 655
125	HAST-RAT[e]	HAST-1: N-hydroxyaryl-amine sulfotransferase	Internal sequence	1297.94	5.89	861.55	32 638
307	HO1_RAT	Heme oxygenase 1	Uncertain; available data from internal sequence	1219.39	5.81	915.71	30 423
413, 1250, 933	HMCS_RAT	HMG CoA synthase, cytosolic	Ab (J. Germershausen)	1033.48	5.59	538.13	54 571
133, 144, 235	HMCS_RAT	HMG CoA synthase, mitochondrial (frag)	Ab (J. Germershausen), *N*-terminal sequence (Steiner/Lottspeich)	666.40	5.02	1019.42	26 811
8, 23, 1307	HS7C_RAT	HSC-70	Positional homology (with human, *etc.*) through coelectrophoresis	811.87	5.27	425.76	69 521
15, 25, 110	P60_RAT	HSP-60	Ab (F. Witzman); confirmed by *N*-terminal sequence and AAA	845.09	5.32	520.03	56 561
971	HS70-RAT[e]	HSP-70	Ab (F. Witzman)	976.11	5.51	437.14	67 674
1216, 1215, 90	HS90-RAT[e]	HSP-90	Ab (F. Witzman)	659.86	5.00	329	90 107
256	INGI-HUMAN	Interferon-γ induced protein	Internal sequence	993.85	5.54	1006.04	27 237
415, 734	LAMB-RAT[e]	Lamin B	Positional homology with human through coelectrophoresis, nuclear location	737.10	5.14	425.19	69 615
80	LAMR-RAT[e]	"Laminin receptor"	Internal sequence	534.02	4.77	697.62	41 327
227	FABL_RAT	L-FABP (liver fatty acid binding protein)	Ab (N. M. Bass)	1586.09	6.18	1483.43	16 622
134	MDHC_MOUSE	Malate dehydrogenase	Internal sequence	1270.85	5.86	861.96	32 620
18, 35, 226	GR75-RAT[e]	Mitcon:3; grp75	Positional homology with human through coelectrophoresis	905.67	5.41	413.67	71 589
175, 251	NCPR_RAT	NADPH P450 reductase	2-D of pure protein	824.69	5.29	393.21	75 366
1168, 1170, 1171	PDI_RAT	PDI: Protein disulfide isomerase	*N*-Terminal sequence (R. M. van Frank), Ab	564.30	4.83	528.47	55 618
47, 93	ALBU_RAT	Pro-Albumin	Microsomal lumen location, p*I*, M_r relative to albumin	1391.03	5.99	446.68	66 195
236	APA1_RAT	Pro-APO A-1 lipoprotein	Coelectrophoresis with plasma protein	920.41	5.43	1137.51	23 467
320	IPK1_BOVIN	Protein kinase C inhibitor 1	Internal sequence; homology with bovine protein	1480.01	6.08	1458.81	17 007
152	PNPH_MOUSE	Purine nucleoside phosphorylase	Internal sequence	1507.19	6.10	911.16	30 599
1179, 1180, 1181, 1182, 1183	PYVC-RAT[e]	Pyruvate carboxylase	Tentative; 2-D of pure protein (J. G. Henslee, *JBC*, 1979); reported in *Biochim. Biophys. Acta 1022*, 115–125.	1485.10	6.08	223.52	131 589
55, 103	SM30_RAT	SMP-30: Senescence marker protein-30	Internal sequence	721.71	5.11	830.10	34 051
135	SODC_RAT	Superoxide dismutase	AAA; comfirmed by internal sequence (R. M. Van Frank)	1161.24	5.74	1388.68	18 173
172	TPM-RAT[e]	Tm: tropomyosin	Location in cytoskeleton, 2-D position relative to human, Ab	476.24	4.66	957.86	28 865
277, 56	TBA1_RAT	Tubulin α	Positional homology with human through coelectrophoresis, cytoskeletal location	688.22	5.06	537.67	54 620
50, 1225	TBB1_RAT	Tubulin β	Positional homology with human through coelectrophoresis, cytoskeletal location	621.29	4.93	535.48	54 855
1224	VIME_RAT	Vimentin	Positonal homology with human through coelectrophoresis, cytoskeletal location	673.00	5.03	539.50	54 426

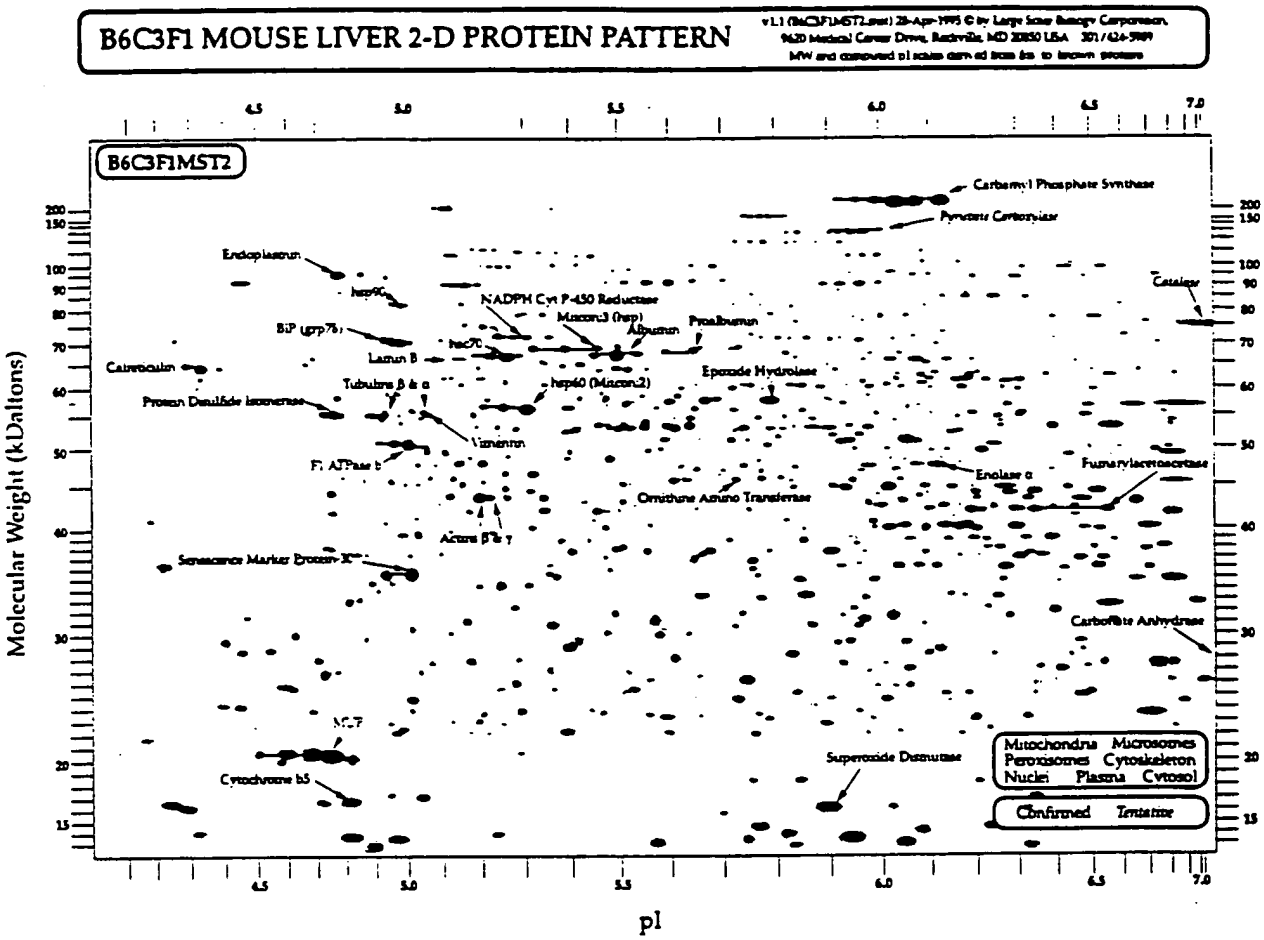

Figure 3. Master 2-D gel pattern for B6C3F1 mouse liver, standardized using the F344 rat liver pattern identifications, according to the method described in the text. Twenty-nine proteins are identified.

$$pI_{RAT\,PLASMA} = f_{RAT\,LIVER\ X\text{–}pI}\left(f_{RAT\,PLASMA\text{–}LIVER\ X\text{–}RAT\,LIVER\ X}\left(f_{RAT\,PLASMA\ X\text{–}RAT\,PLASMA\text{–}LIVER\ X}\left(X_{RAT\,PLASMA}\right)\right)\right) \quad (8)$$

This unified approach, in which one well-populated 2-D pattern is used to standardize a family of other patterns, has the additional advantage that the resulting p*I* and M_r scales are directly compatible. Hence one can compare the relative p*I*'s of mouse and rat versions of a sequenced protein in a consistent p*I* measurement system, and select likely inter-species analogs based on positional relationships on common scales. Adoption of immobilized pH gradient (IPG) technology [4–7] will result in substantial improvements in p*I* positional reproducibility for standard 2-D maps such as those presented here; however, we believe that our approach will continue to be useful in establishing the empirical pH gradient actually achieved by such gels under given experimental conditions (temperature, urea concentration, *etc.*), in relating patterns run on different IPG ranges and using different lots of IPG gels (between which some variation will persist). Development of rodent organ maps is a continuing effort in our laboratories [8–10], and results in regular additions of identified proteins. Those who wish to receive current rodent liver maps, with color annotations, should send a stamped self-addressed envelope to the first author.

We would like to thank the individuals who provided antibodies mentioned in Table 1, and R. M. van Frank for unpublished sequenced data.

Received May 31, 1995

References

[1] Anderson, N. L., Esquer-Blasco, R., Hofmann, J.-P., Anderson, N. G., *Electrophoresis* 1991, *12*, 907–930.
[2] Rosenfeld, J., Capdevielle, J., Guillemot, J. C., Ferrara, P., *Anal. Biochem.* 1992, *203*, 173–179.
[3] Witzmann, F., Clack, J., Fultz, C., Jarnot, B., *Electrophoresis* 1995, *16*, 451–459.
[4] Rosengren, A. E., Bjellqvist, B., Gasparic, V., *US Patent* 4130470, December 1978.
[5] Gianazza, E., Artoni, G., Righetti, P. G., *Electrophoresis* 1983, *4*, 321–326.
[6] Görg, A., Postel, W., Günther, S., Weser, J., *Electrophoresis* 1985, *6*, 599–604.
[7] Gianazza, E., Astrua-Testori, S., Giacon, P., Righetti, P. G., *Electrophoresis* 1985, *6*, 332–339.
[8] Myers, T. G., Dietz, E. C., Anderson, N. L., Khairallah, E. A., Cohen, S. D., Nelson, S. D., *Chem. Res. Toxicol.* 1995, *8*, 403–413.
[9] Cunningham, M. L., Pippin, L. L., Anderson, N. L., Wenk, M. L., *Toxicol. Appl. Pharmacol.* 1995, *131*, 216–223.
[10] Anderson, N. L., Copple, D. C., Bendele, R. A., Probst, G. S., Richardson, F. C., *Fundam. Appl. Toxicol.* 1992, *18*, 570–580.

2

Progress with Proteome Projects: Why all Proteins Expressed by a Genome Should be Identified and How To Do It

MARC R. WILKINS[1], JEAN-CHARLES SANCHEZ[2], ANDREW A. GOOLEY[1], RON D. APPEL[3], IAN HUMPHERY-SMITH[2], DENIS F. HOCHSTRASSER[3] AND KEITH L. WILLIAMS[1,*]

[1] *Macquarie University Centre for Analytical Biotechnology, Macquarie University, Sydney, NSW 2109, Australia;* [2] *Department of Microbiology, University of Sydney, NSW, 2006, Australia and* [3] *Central Clinical Chemistry Laboratory and Medical Computing Centre of the University of Geneva, CH 1211 Geneva 14, Switzerland*

Introduction

The advent of large genome sequencing projects has changed the scale of biology. Over a relatively short period of time, we have witnessed the elucidation of the complete nucleotide sequence for bacteriophage λ (Sanger *et al.*, 1982), the nucleotide sequence of an eukaryotic chromosome (Oliver *et al.*, 1992), and in the near future will see the definition of all open reading frames of some simple organisms, including *Mycoplasma pneumoniae*, *Escherichia coli*, *Saccharomyces cerevisiae*, *Caenorhabditis elegans* and *Arabidopsis thaliana*. Nevertheless, genome sequencing projects are not an end in themsleves. In fact, they only represent a starting point to understanding the function of an organism. A great challenge that biologists now face is how the co-expression of thousands of genes can best be examined under physiological and pathophysiological conditions, and how these patterns of expression define an organism.

There are two approaches that can be used to examine gene expression on a large scale. One uses nucleic acid-based technology, the other protein-based technology. The most promising nucleic-acid based technology is differential display of mRNA (Liang and Pardee, 1992; Bauer *et al.*, 1993), which uses polymerase chain reaction with arbitrary primers to generate thousands of cDNA species, each which correspond to an expressed gene or part of a gene. However, it is currently unclear if this technique can be developed to reliably assay the expression of thousands of genes or

* Corresponding Author

Biotechnology and Genetic Engineering Reviews – Vol. 13, December 1995
0264–8725/94/12/1–38 $20.00 + $0.00

identify all cDNA species, and the approach does not easily allow a systematic screening. Analysis of gene expression by the study of proteins present in a cell or tissue presents a favorable alternative. This can be achieved by use of two-dimensional (2-D) gel electrophoresis, quantitative computer image analysis, and protein identification techniques to create 'reference maps' of all detectable proteins. Such reference maps establish patterns of normal and abnormal gene expression in the organism, and allow the examination of some post-translational protein modifications which are functionally important for many proteins. It is possible to screen proteins systematically from reference maps to establish their identities.

To define protein-based gene expression analysis, the concept of the 'proteome' was recently proposed (Wilkins *et al.*, 1995; Wasinger *et al.*, 1995). A proteome is the entire PROTein complement expressed by a genOME, or by a cell or tissue type. The concept of the proteome has some differences from that of the genome, as while there is only one definitive genome of an organism, the proteome is an entity which can change under different conditions, and can be dissimilar in different tissues of a single organism. A proteome nevertheless remains a direct product of a genome. Interestingly, the number of proteins in a proteome can exceed the number of genes present, as protein products expressed by alternative gene splicing or with different post-translational modifications are observed as separate molecules on a 2-D gel. As an extrapolation of the concept of the 'genome project', a 'proteome project' is research which seeks to identify and characterise the proteins present in a cell or tissue and define their patterns of expression.

Proteome projects present challenges of a similar magnitude to that of genome projects. Technically, the 2-D gel electrophoresis must be reproducible and of high resolution, allowing the separation and detection of the thousands of proteins in a cell. Low copy number proteins should be detectable. There should be computer gel image analysis systems that can qualitatively and quantitatively catalog the electrophoretically separated proteins, to form reference maps. A range of rapid and reliable techniques must be available for the identification and characterisation of proteins. As a consequence of a proteome project, protein databases must be assembled that contain reference information about proteins; such databases must be linked to genomic databases and protein reference maps. Databases should be widely accessible and easy to use.

Recently, there have been many changes in the techniques and resources available for the analysis of proteomes. It is the aim of this chapter to discuss the status of the areas outlined above, and to review briefly the progress of some current proteome projects.

Two-dimensional electrophoresis of proteomes

Two dimensional (2-D) gel electrophoresis involves the separation of proteins by their isoelectric point in the first dimension, then separation according to molecular weight by sodium dodecyl sulfate electrophoresis in the second dimension. Since first described (Klose, 1975; O'Farrell, 1975; Scheele, 1975), it has become the method of choice for the separation of complex mixtures of proteins, albeit with many modifications to the original techniques. 2-D electrophoresis forms the basis of proteome projects through separating proteins by their size and charge (Hochstrasser *et al.*,

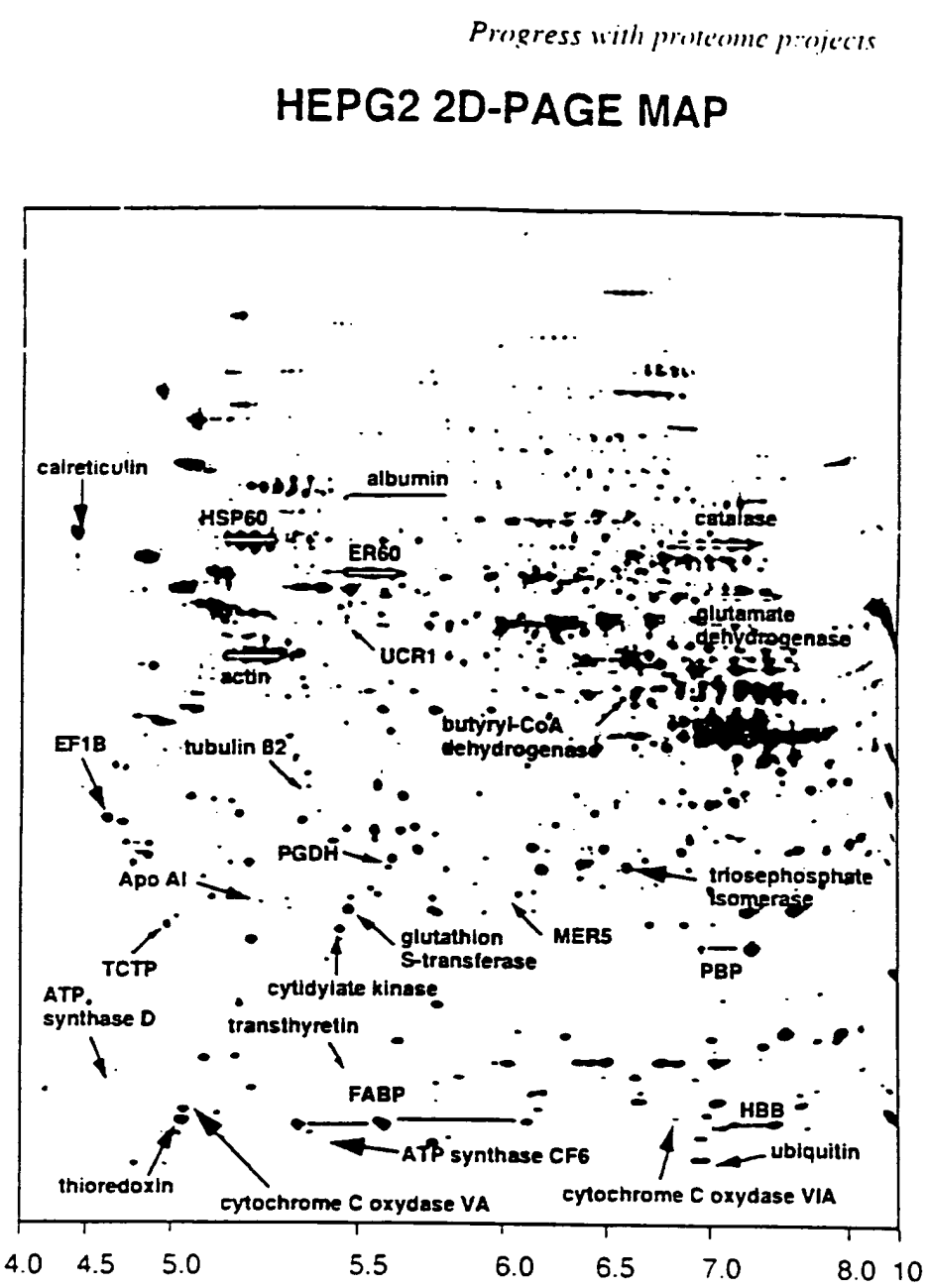

Figure 1. Two-dimensional gel electrophoresis map of a human hepatoblastoma-derived cell line, illustrating the very high resolution of the technique. The first dimensional separation (right to left of figure) was achieved using immobilised pH gradient electrophoresis of 4.0 to 10.0 units. The second dimension (top to bottom of figure) was SDS-PAGE using a 11%–14% acrylamide gradient, allowing separation in the molecular weight range 10–250 kDa. Proteins were visualised by silver staining. Arrows show proteins of known identity.

1992; Celis *et al.*, 1993; Garrels and Franza, 1989; VanBogelen *et al.*, 1992). Current protocols can resolve two to three thousand proteins from a complex sample on a single gel (*Figure 1*).

2-D GEL RESOLUTION AND REPRODUCIBILITY

A primary challenge of separating complex mixtures of proteins by 2-D gel electrophoresis has been to achieve high resolution and reproducibility. High resolution ensures that a maximum of protein species are separated, and high reproducibility is

vital to allow comparison of gels from day to day and between research sites. These factors can be difficult to achieve.

Carrier ampholytes are a common means of isoelectric focusing for the first dimension of 2-D electrophoresis. Gels are usually focused to equilibrium to separate proteins in the pI range 4 to 8, and run in a non-equilibrium mode (NEPHGE) to separate proteins of higher pI (7 to 11.5) (O'Farrell, 1975; O'Farrell, Goodman and O'Farrell, 1977). Unfortunately, the use of carrier ampholytes in the isoelectric focusing procedure is susceptible to 'cathode drift', whereby pH gradients established by prefocusing of ampholytes slowly change with time (Righetti and Drysdale, 1973). Carrier ampholyte pH gradients are also distorted by high salt concentration of samples (Bjellqvist *et al.*, 1982), and by high protein load (O'Farrell, 1975). A further limitation is that iso electric focusing gels, which are cast and subject to electrophoresis in narrow glass tubes, need to be extruded by mechanical means before application to the second dimension – a procedure that potentially distorts the gel. Nevertheless, many of the above shortcomings can be avoided by loading small amounts of ^{14}C or ^{35}S radiolabelled samples (Garrels, 1989; Neidhardt *et al.*, 1989; Vandekerkhove *et al.*, 1990). High sensitivity detection is then achieved through use of fluorography or phosphorimaging plates (Bonner and Laskey, 1974; Johnston, Pickett and Barker, 1990; Patterson and Latter, 1993). However, this approach is only practicable for organisms or tissues that can be radiolabelled.

An alternative technique, which is becoming the method of choice for the first dimension separation of proteins, involves isoelectric focusing in immobilized pH gradient (IPG) gels (Bjellqvist *et al.*, 1982; Görg, Postel and Gunther, 1988; Righetti, 1990). Immobilized pH gradients are formed by the covalent coupling of the pH gradient into an acrylamide matrix, creating a gradient that is completely stable with time. IPG gels are usually poured onto a stiff backing film, which is mechanically strong and provides easy gel handling (Ostergren, Eriksson and Bjellqvist, 1988). The major advantages of IPG separations are that they do not suffer from cathodic drift, they allow focusing of basic and very acidic proteins to equilibrium, pH gradients can be precisely tailored (linear, stepwise, sigmoidal), and that separations over a very narrow pH range are possible (0.05 pH units per cm) (Righetti, 1990; Bjellqvist *et al.*, 1982, 1993a; Sinha *et al.*, 1990; Görg *et al.*, 1988; Gelfi *et al.*, 1987; Gunther *et al.*, 1988). However, it is not currently possible to use IPG gels to separate very basic proteins of isoelectric point greater than 10, although this is under development. Narrow pH range separations are useful to address problems of protein co-migration in complex samples, allowing 'zooming in' on regions of a gel (*Figure 2*). IPG gel strips are now commercially available, which begin to address the problems of intra- and inter-lab isoelectric focusing reproducibility.

There are two means of electrophoresis for the second dimension separation of proteins: vertical slab gels and horizontal ultrathin gels (Görg, Postel, and Gunther, 1988). Both are usually SDS-containing gradient gels of approximately 11% to 15% acrylamide, which separate proteins in the molecular mass range of 10 – 150kD. A stacking gel is not usually used with slab gels, but is necessary when using horizontal gel setups (Görg, Postel and Gunther, 1988). Comparisons have shown that there is little or no difference in the reproducibility of electrophoresis using either approach (Corbett *et al.*, 1994a), but commercially available vertical or horizontal precast gels will provide greater reproducibility for occasional users. For slab gel electrophoresis,

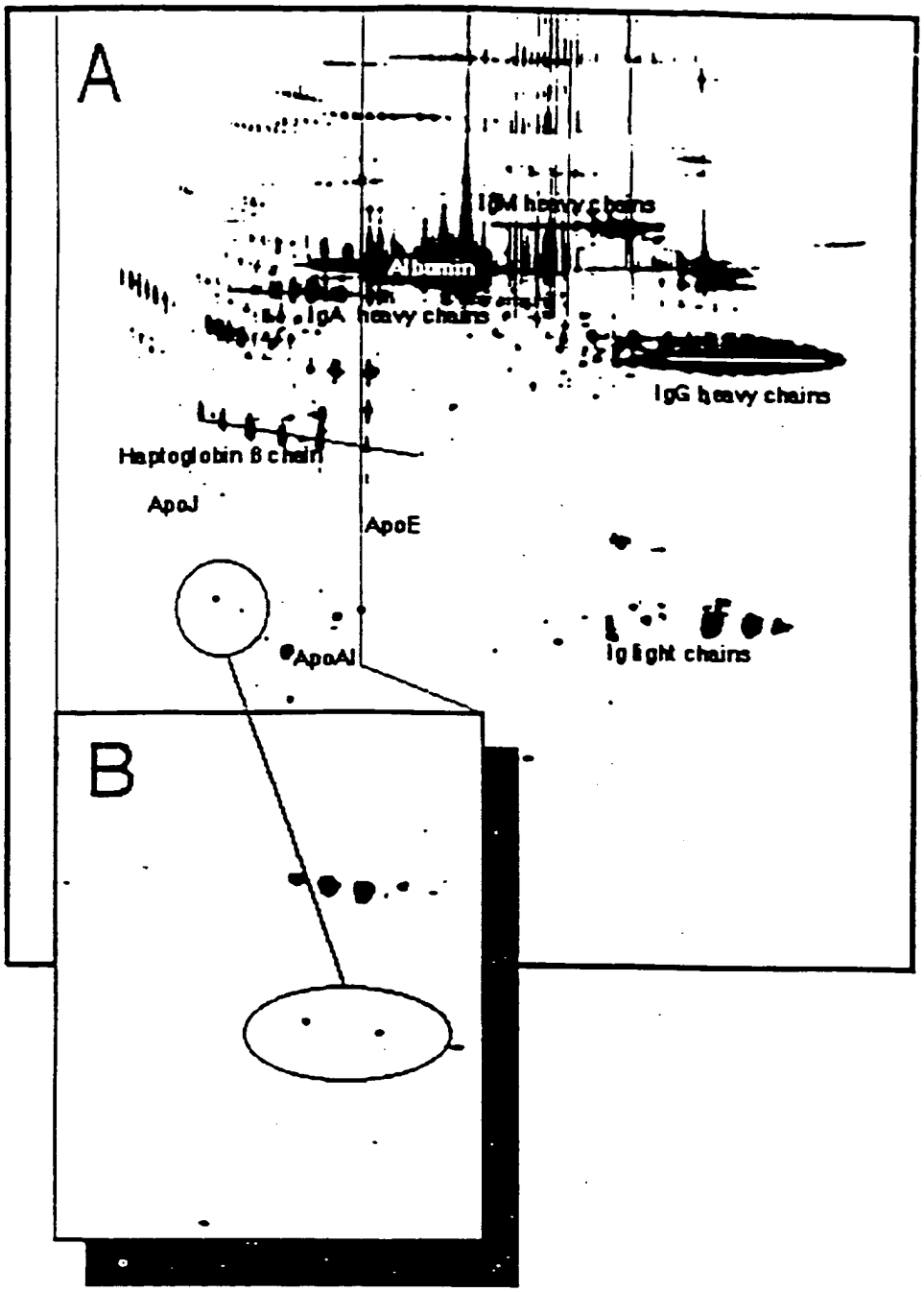

Figure 2. Two-dimensional gel electrophoresis allows 'zooming in' on areas of interest. Rings highlight 2 proteins common to each gel. (A) Wide pI range two dimensional electrophoresis map of human plasma proteins. First dimension separation was acheived using an immobilised pH gradient of 3.5 to 10.0 units. The second dimension was SDS-PAGE. Actual gel size was 16cm × 20cm, and proteins were visualised with silver staining. (B) Narrow pI range electrophoresis was used to 'zoom in' on a small region of the plasma map. The first dimension used a narrow range immobilised pH gradient of 4.2 to 5.2 units, and second dimension was SDS-PAGE. Micropreparative loading was used, and the gel blotted to PVDF. Proteins were visualised with amido black. Actual blot size was 16cm × 20cm.

the use of piperazine diacrylyl as a gel crosslinker and the addition of thiosulfate in the catalyst system has been shown to give better resolution and higher sensitivity detection (Hochstrasser and Merril, 1988; Hochstrasser, Patchornik and Merril, 1988).

Notwithstanding the advances described above, there is an increasing demand to improve the reproducibility of 2-D electrophoresis to facilitate database construction and proteome studies. Harrington *et al.* (1993) explain that if a gel resolves 4000 protein spots, and there is 99.5% spot matching from gel to gel, this will produce 20 spot errors per gel. This amount of error, which might accumulate with each gel to gel comparison used in database construction, could produce an unacceptable degree of uncertainty in gel databases. To address these issues, partial automation of large 2-D gel separations has been undertaken (Nokihara, Morita and Kuriki, 1992; Harrington *et al.*, 1993). Although results are preliminary, spot to spot positional reproducibility in one study was found to be threefold improved over manual methods (Harrington *et al.*, 1993). It should be noted that small 2-D gel formats (50 × 43 mm) have been almost completely automated (Brewer *et al.*, 1986), although these are not generally used for database studies.

MICROPREPARATIVE 2-D GEL ELECTROPHORESIS

With the advent of affordable protein microcharacterisation techniques, including N-terminal microsequencing, amino acid analysis, peptide mass fingerprinting, phosphate analysis and monosaccharide compositional analysis, a new challenge for 2-D electrophoresis has been to maintain high resolution and reproducibility but to provide protein in sufficient quantities for chemical analysis (high nanogram to low microgram quantities of proteins per spot). This becomes difficult to achieve with very complex samples such as whole bacterial cells, as the initial protein load is divided among 2000 to 4000 protein species. Two approaches are used for producing amounts of material that can be chemically characterised. The first method is to run multiple gels, collect and pool the spots of interest, and subject them to concentration (Ji *et al.*, 1994; Walsh *et al.*, 1995; Rasmussen *et al.*, 1992). In this approach, the concentration process must also act as a purification step to remove accumulated electrophoretic contaminants such as glycine. A more elegant approach has been to exploit the high loading capacity of IPG isoelectric focusing. The high loading capacity of immobilised pH gradients was described early (Ek, Bjellqvist and Righetti, 1983), but has only recently been applied to 2-D electrophoresis (Hanash *et al.*, 1991; Bjellqvist *et al.*, 1993b). Up to 15 mg of protein can been applied to a single gel, yielding microgram quantities of hundreds of protein species. A further benefit of this approach is that proteins present in low abundance, which may not be visualised by lower protein loads, are more likely to be detected. The use of electrophoretic or chromatographic prefractionation techniques (Hochstrasser *et al.*, 1991a; Harrington *et al.*, 1992), followed by high loading of narrow-range IPG separations (Bjellqvist *et al.*, 1993b) provides a likely solution to studies on proteins present in low abundance.

Methods of protein detection

There are many means for detecting proteins from 2-D gels. The method used will be dictated by factors including protein load on gel (analytical or preparative), the purpose of the gel (for protein quantitation or for blotting and chemical characterisation), and the sensitivity required. The most common means of protein detection and their applications are shown in *Table 1*. Most detection methods have drawbacks, for

Table 1: Common stains for 2-D gels or blots and their applications.

Detection Method	Main applications	Unsuitable applications	Sensitivity	References
[^{35}S] Met or ^{14}C radiolabelling and fluorography or phosphorimaging	Cell lines, cultured organisms	Samples that cannot be labelled	20 ppm of radiolabel in a spot	Garrels and Franza, 1989; Latham, Garrels and Soltier, 1993
[^{35}S]thiourea silver	Extremely high sensitivity gel staining	Preparative 2-D; PVDF or NC membranes	0.4 ng protein on spot or band of gel	Wallace and Saluz, 1992a,b
Silver	Very high sensitivity gel staining, can be mono or polychromatic	Preparative 2-D; PVDF or NC membranes	4 ng protein on spot or band of gel	Rabilloud, 1992; Hochstrasser and Merril, 1988
Coomassie blue R-250	Staining of gels; staining of PVDF membranes before protein sequencing	Staining prior to direct mass determination from PVDF; amino acid analysis on PVDF; detection of some glycoproteins	40 ng protein on band or spot of gel	Strupat *et al.*, 1994; Gharahdaghi *et al.*, 1992; Goldberg *et al.*, 1988; Sanchez *et al.*, 1992
Colloidal gold	Staining NC membranes, staining PVDF before direct MALDI-TOF	Gels	60 × higher than coomassie	Yamaguchi and Asakawa, 1988; Eckerskorn *et al.*, 1992; Strupat *et al.*, 1994
Zinc imidazole	Reverse staining of gels or membranes; may be beneficial in MALDI-TOF of peptides	Where positive image is required	Higher than coomassie	Ortiz *et al.*, 1992; James *et al.*, 1993
Ponceau S and amido black	Staining higher protein loads on PVDF, for protein sequencing or amino acid analysis	Staining prior to direct mass determination from PVDF	100 ng protein on band or spot of gel	Sanchez *et al.*, 1992; Strupat *et al.*, 1994; Wilkins *et al.*, 1995.
India ink	Staining of membrane-bound proteins; staining PVDF before direct MALDI-TOF	Gel staining; not quantitative from protein to protein	1–10 ng	Li *et al.*, 1989; Hughes, Mack and Hamparian, 1988; Strupat *et al.*, 1994
Stains-all	Staining to detect glycoproteins or Ca^{2+} binding proteins	General gel staining	100 ng protein on band or spot of gel	Campbell, MacLennan and Jorgensen, 1983; Goldberg *et al.*, 1988

PVDF = polyvinylidene difluoride, NC = nitrocellulose, MALDI-TOF = matrix assisted laser desorption ionisation time of flight mass spectrometry.

example, some glycoproteins are not stained by coomassie blue (Goldberg *et al.*, 1988), and many organic dyes are unsuitable for protein detection on PVDF if samples are to be used for direct matrix-assited laser desorption ionisation mass spectrometry (Strupat *et al.*, 1994).

Although most means of protein detection give some indication of the quantities of protein present, in general they cannot be used for global quantitation. This is because

no protein stain is able consistently to detect proteins over a wide range of concentrations, isoelectric points and amino acid compositions, and with a variety of post-translational modifications (Goldberg *et al.*, 1988; Li *et al.*, 1989). Furthermore, there are large differences in staining pattern when identical gels or blots are subjected to different stains, including amido black, imidazole zinc, india ink, ponceau S, colloidal gold, or coomassie blue (Tovey, Ford and Baldo, 1987; Ortiz *et al.*, 1992). The most common means of quantitating large numbers of proteins in a 2-D gel involves the radiolabelling of protein samples prior to electrophoresis, and protein quantitation based on fluorography and image analysis or liquid scintillation counting (Garrels, 1989; Celis and Olsen, 1994). However, proteins which do not contain methionine cannot be detected if only [^{35}S] methionine is used for labelling. Amino acid analysis of protein spots visualised by other techniques presents a likely means of protein quantitation for the future.

BLOTTING OF PROTEINS TO MEMBRANES

Electrophoretic blotting of proteins from two-dimensional polyacrylamide gels to membranes presents many options for protein identification and microcharacterisation which are not possible when proteins remain in gels. For example, when proteins are blotted to polyvinylidene difluoride (PVDF) membranes, they can be identified by N-terminal sequencing, amino acid analysis, or immunoblotting, or they may be subjected to endoproteinase digestion, monosaccharide analysis, phosphate analysis, or direct matrix-assisted laser desorption ionisation mass spectrometry (Matsudaira, 1987; Wilkins *et al.*, 1995; Jungblut *et al.*, 1994; Sutton *et al.*, 1995; Rasmussen *et al.*, 1994; Weizthandler *et al.*, 1993; Murthy and Iqbal, 1991; Eckerskorn *et al.*, 1992). It is possible to combine of some of these procedures on a single protein spot on a PVDF membrane (Packer *et al.*, 1995; Wilkins *et al.*, submitted; Weizthandler *et al.*, 1993). This is useful when minimal amounts of protein are available for analysis. These techniques will be explored in detail later in this review. Notwithstanding the above, there are some disadvantages associated with blotting of proteins to membranes. There is always loss of sample during blotting procedures (Eckerskorn and Lottspeich, 1993), and common protein detection methods are less sensitive or not applicable to membranes (*Table 1*), presenting difficulties for the analysis of low abundance proteins. Detailed discussion of the merits of available membranes and common blotting techniques can be found elsewhere (Eckerskorn and Lottspeich, 1993; Strupat *et al.*, 1994; Patterson, 1994).

2-D gel analysis, documentation, and proteome databases

Following protein electrophoresis and detection, detailed analysis of gel images is undertaken with computer systems. For proteome projects, the aim of this analysis is to catalogue all spots from the 2-D gel in a qualitative and if possible quantitative manner, so as to define the number of proteins present and their levels of expression. Reference gel images, constructed from one or more gels, form the basis of two-dimensional gel databases. These databases also contain protein spot identities and